Tutor/s

Dr. Rodrigo Soto
Dra. Eliana Ramírez
Departament of Chemical Engineering
and Analytical Chemistry

Grau en
Enginyeria
Química

-

Treball Final de Grau

Contribution to the kinetic study of the dehydration of sorbitol over acidic ion-exchange resins.

Eric Quinto Fernández

June 2022

UNIVERSITAT DE
BARCELONA

Aquesta obra està subjecta a la llicència de:
Reconeixement–NoComercial-SenseObraDerivada

http://creativecommons.org/licenses/by-nc-nd/3.0/es/

Fix your course on a star and you'll navigate any storm.

Leonardo da Vinci

.

En primer lugar, me gustaría agradecer especialmente a mi tutor, el Dr. Rodrigo Soto, por haberme dedicado tanto tiempo, ayuda, apoyo e, incluso, alguna que otra carcajada. Ha conseguido que este proyecto sea muy ameno y me ha proporcionado una visión mucho más amplia de lo que significa ser ingeniero. Gracias también a mi tutora, la Dra. Eliana Ramírez, por el apoyo ofrecido durante el proyecto y por todo lo que he podido aprender de ella a lo largo de los años de carrera.

Por otro lado, agradecer a mis compañeros de laboratorio Sandra, Mónica, Marc, Eloi y Jose por convertir el largo tiempo entre muestras en unos momentos mucho más entretenidos y por ayudarme en la experimentación cuando la compaginaba con ir a clase.

A su vez, dar las gracias a mis compañeros más cercanos de la carrera, los cuáles si leen este texto se darán por aludidos, por el apoyo y confianza brindados durante estos últimos años y por haber estado a mi lado en todo momento. Probablemente sin ellos llegar hasta aquí no hubiese sido posible. Espero de corazón que triunféis allá donde vayáis.

Además, como olvidar a mis compañeros de piso Mar, Marc y David que me han acompañado en mis decepciones y mis alegrías durante este último año y que se han preocupado por mi y por el avance de este proyecto desde que lo empecé.

Finalmente, a mi familia, especialmente a mi madre que, aunque estuviésemos un poco alejados, nunca ha dejado de darme los ánimos, la ayuda y la confianza que he necesitado para sacar este trabajo adelante.

CONTENTS

SUMMARY

Currently, the use of petroleum derivatives as a base in the commodity and fuel industry poses environmental and economic disadvantages of real concern. Therefore, the search for a substitute that can satisfy the current demands for this form of energy in a sustainable and cost-effective way has become a focus of global attention and research. Biomass, a green source of organic and plant-based resources, has proven to be a very promising candidate.

Specifically, isosorbide is one of the molecules from biomass that has been gaining interest over the years. Nowadays, it is used in industrial processes in the pharmaceutical and cosmetics sectors, but its most important application is in the manufacture of polymers due to its appreciable rigidity in its structure.

The most commonly used process to obtain this compound consists of a double dehydration of sorbitol to 1,4-sorbitan, the intermediate product, and from this to isosorbide. Sorbitol is a polyol that is quite common in nature and with a high market value. The reaction is carried out using an acid catalyst, currently sulphuric acid, which generates several drawbacks, such as corrosion of the devices used and a large expenditure of energy. Therefore, there is a desire to find solid catalysts able to overcome all these obstacles while providing good performance values and efficient isosorbide production.

Several solid catalysts have already been investigated, e.g. ion exchange resins have been shown to be viable catalysts in this process, especially CT-482 offering high yield values at 190ºC.

In this work, an analysis of the conditions under which the effects of catalyst loading, and internal and external mass transfers can be considered negligible is carried out by means of a set of preliminary experiments. Under such conditions, the kinetics of sorbitol dehydration was studied at different initial reactant concentrations and temperatures. As a result, activation energies of 90 ± 10 kJ/mol were obtained for the consumption of sorbitol and 100 ± 18 kJ/mol for the formation of isosorbide, the latter being the rate-controlling step of the reaction.

In addition, an empirical modelling of the rate of isosorbide formation as a function of temperature and initial amount of reactant was performed. It was observed that the influence of the former is clearly much more dominant than the latter. However, a trend was shown that if one dependent variable increased, the effect of the other on the response variable was significantly higher.

Keywords:

Sorbitol, isosorbide, ion-exchange resins, mass transfer resistances, reaction kinetics

RESUMEN

Actualmente, el uso de los derivados del petróleo como base en la industria de productos básicos y combustibles supone unos inconvenientes medioambientales y económicos realmente preocupantes. Por ello, la búsqueda de un sustituto que pueda atender las demandas actuales de esta forma de energía mediante una vía sostenible y rentable se ha convertido en un centro de atención e investigación a nivel mundial. La biomasa, una fuente verde de recursos de origen orgánico y vegetal, ha demostrado ser un candidato muy prometedor.

En concreto, la isosorbida es una de las moléculas provenientes de la biomasa que ha ido incrementando interés con el paso de los años. Hoy en día, es empleada en procesos industriales en los sectores de la farmacéutica y la cosmética, pero la fabricación de polímeros es su aplicación más destacada debido a su apreciable rigidez en su estructura.

El proceso de obtención más usado de este compuesto consta de una doble deshidratación de sorbitol a 1,4-sorbitan, el producto intermedio, y de este a isosorbida. El sorbitol es un polialcohol bastante común en la naturaleza y con un gran índice de mercado. La reacción se lleva a cabo empleando un catalizador ácido, actualmente ácido sulfúrico, generando varios inconvenientes, así como la corrosión de los dispositivos utilizados y un gran gasto energético. Debido a ello, se desean encontrar catalizadores sólidos que pongan fin a todos estos obstáculos y que, además, proporcionen buenos valores de rendimiento y producción de isosorbida de manera eficiente.

Ya han sido investigados varios catalizadores sólidos como, por ejemplo, las resinas de intercambio iónico que han demostrado ser viables catalizadores en este proceso, especialmente la CT-482 ofreciendo valores de rendimiento elevados a 190ºC.

En este trabajo se realiza un análisis de las condiciones en las que los efectos de la carga del catalizador y las transferencias de masa internas y externas pueden considerarse despreciables mediante un conjunto de experimentos preliminares. En tales condiciones, se estudió la cinética de la deshidratación del sorbitol a diferentes concentraciones iniciales de reactivos y temperaturas. Como resultado, se obtuvieron energías de activación de 90 ± 10 kJ/mol para el consumo de sorbitol y 100 ± 18 kJ/mol para la formación de isosorbida, siendo esta última la etapa que controla la velocidad de la reacción.

Además, se realizó una modelización empírica de la velocidad de formación de isosorbida en función de la temperatura y de la cantidad inicial de reactante. Se observó que la influencia de la primera variable es claramente mucho más dominante que la segunda. Sin embargo, se mostró una tendencia según la cual, si una de las variables dependientes aumentaba, el efecto de la otra sobre la variable de respuesta era significativamente mayor.

Palabras clave: Sorbitol, isosorbida, resinas de intercambio iónico, resistencias de transferencia de masa, cinética de reacción

INTRODUCTION

1.1. RENEWABLE ENERGY SOURCE: BIOMASS

Renewable energy sources are growing in importance due to the environmental impact caused by the use of petroleum derivatives as feedstock in today's society. Among them, biomass is the only one capable of providing an economical, viable and green production of carbon, which is used in most fuels and consumer goods today.

The development of this form of energy therefore means means moving progressively closer to substituting petroleum derivatives in the production of commodities and a wide range of chemicals, as well as improving energy security in areas without abundant fossil fuels, increasing the supply of liquid fuels used for transport and reducing net carbon emissions to the atmosphere [1]. This last aspect influences the planet by decreasing its atmospheric pollution, reducing the acidification of its oceans, and not contributing to global warming, also known as the greenhouse effect. However, biomass is not only used to produce fuels, but also for electricity generation, home heating or for the supply of heat for some industrial processes.

Biomass consists of carbohydrate plant material resulting from photosynthesis in vegetation. Several researchers have defined different types of biomasses in various ways. One of them is according to their origin which can be: woody plants, herbaceous plants, aquatic plants and dung, of which the first two are the most widely studied.

More internally, biomass is made up of a mixture of varying amounts of cellulose, hemicellulose, lignin and a small amount of other extractives. Slow growth and a tightly bound structure are characteristics of woody plants, while herbaceous plants, having a looser structure, give a clue that their lignin content is lower. It is therefore logical that the relative proportion of cellulose and lignin is an important factor in determining the appropriateness of plant species for further processing as energy crops [2]. Other properties that may be crucial depending on the energy conversion process are also moisture content, calorific value or the proportions of fixed and volatile carbons, among others.

1.2. DEHYDRATION OF SORBITOL TO ISOSORBIDE

1.2.1. Sorbitol

Sorbitol ($C_6H_{14}O_6$), also called D-glucitol, is a polyalcohol formed by 6 carbon atoms and 6 hydroxyl groups as shown in *Figure 1*.

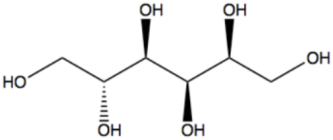

Figure 1. Sorbitol chemical structure

It was discovered in 1872 by the French chemist Jean-Baptiste Bossingault in the berries of a common European deciduous tree called Sorbus aucuparia L. However, it is commonly found naturally in other fruits and berries. In terms of industrial processes, the catalytic hydrogenation of the monosaccharide D-glucose is the most widely used for obtaining this polyol[3] although the electrochemical reduction of D-glucose [4] and the bioconversion of fructose by the bacterium Zymomonas Mobilis [5] are also noteworthy.

After many years of commercialisation, sorbitol has become a commodity with an annual production of 2000kt and a market price of between 0.55 to 0.65 USD/kg. Personal care, cosmetics, diabetic and dietetic food, pharmaceuticals and chemicals are examples of industries that benefit from the uses of this raw material [6]. The latter in particular has gained much interest since the US Department of Energy recognised sorbitol as one of the top 12 carbohydrate-derived chemicals that could be used as a chemical platform in 2004 [7]. Following a review in 2010, this compound is still included in this list of potential pioneers [8]. If it is added the current global trend of replacing petroleum derivatives with biomass derivatives in the production of commodities and intermediates, it is obvious how this polyol has emerged as a focus of attention in modern research.

Today, the typically commercial form of sorbitol corresponds to 70% aqueous syrup, but it is also commonly found as a pure solid. In this state, it is characterised as a white crystalline compound, soluble in water and odourless.

1.2.2. Isosorbide

Isosorbide ($C_6H_{10}O_4$) is a V-shapped chiral diol composed of two cis-fused tetrahydrofuran units with two secondary alcohols as shown in *Figure 2*. The hydroxyl group of the C5 carbon is located in endo position (inside the V-shape) and is more sterically protected than the other hydroxyl group which is located in exo position (away from the THF). Therefore, the acidity and reactivity of the functional groups are different due to the heterogeneous configuration.

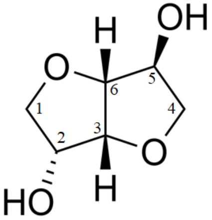

Figure 2. Isosorbide chemical structure

The interest of isosorbide in terms of industrial processes lies in the manufacture of isosorbide nitrates used as vasodilators, the preparation of cosmetic or pharmaceutical solutions and, especially, in the synthesis of polymers [9] due to the interesting rigidity provided by its own structure, its chirality and its harmlessness. Moreover, from an environmental point of view, isosorbide is considered a biobased platform molecule as it has the potential to become an alternative to many petro-derived compounds. The substitution of bisphenol-A in the production of polycarbonates and epoxy resins proves to be an enlightening example. For these reasons, its marketability has become more and more popular over the years, reaching a global market of about 430 million USD in 2019 and is estimated to grow by up to 40% by 2025 [10].

However, the yields and selectivities obtained so far in the fabrication of such a compound are below the standards for industrial production. Given the promising qualities and various applications of isosorbide today, the search for a cost-effective and efficient synthesis process for the compound has become an object of desire worldwide.

1.2.3. Mechanism of the dehydration sorbitol reaction

The isosorbide (IB) synthetic process is composed of a two-step reaction mechanism in which a double dehydration of sorbitol (SOH) takes place. However, in the first dehydration, several by-products can be formed that can negatively affect the yield and selectivity of the isosorbide, since the only intermediates that can lead to its production are 3,6- and 1,4-sorbitan (1,4-STAN), as illustrated in *Figure 3*.

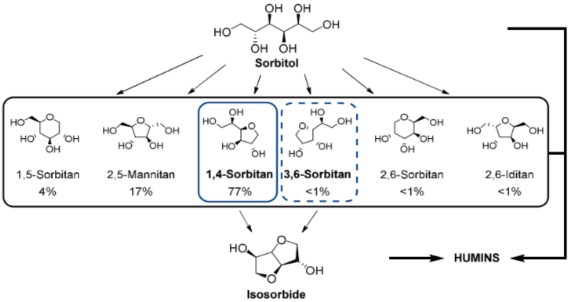

Figure 3. Synthesis of the isosorbide reaction mechanism [11]

These two species differ in terms of which of the two rings that constitute the isosorbide is formed first: the cycle formed by the carbons at positions 1 and 4 or, conversely, with the C3 and C6 carbons, with a much higher formation of the former [11]. This mechanism consists of an SN2 substitution reaction in which the hydroxyl group of C1 is protonated and leaves the structure as a water molecule, due to the interaction with the hydroxyl of C4. In this way, one of the furan rings is formed [12].

As for the by-products generated, 2,5-sorbitan (2,5-STAN) forms a large part of the range, the rest being found in negligible quantities. In addition, it is common that in the course of carbohydrate dehydration reactions, products are formed as a result of the degradation and condensation of some of the compounds present. This set of polymeric structures is often referred to as "humins" and usually have a characteristic dark brown colour. This phenomenon represents one of the limitations of isosorbide production at the industrial level [11].

At present, the industrial process of sorbitol dehydration is carried out using sulphuric acid as a catalyst providing high sorbitol conversions at low temperature but entailing serious economic and environmental problems [13]. Complex separation of the isosorbide from the reaction medium, corrosion of the equipment and production of residual acid are some of the previously mentioned drawbacks.

In order to prevent these obstacles, this reaction has been investigated by solid catalysis such as sulphated metal oxides [14], zeolites [15] or sulfonic acid resins [16]. In particular, ion exchange resins have proven to be a promising and efficient option for the sorbitol dehydration reaction, obtaining high conversion and yield values at relatively low temperatures as shown in *Table 1*, especially over Purolite CT-482.

TABLE 1. Summary table of experimental results carried out at the same conditions with different resins (T=170ºC, t=8.5h, m^0_{SOH}=4.50 g, wcat=1.00 g, stirring=750 rpm) [17]

	X [%]	S [%]			Y [%]		
	SOH	IB	1,4-STAN	2,5-STAN	IB	1,4-STAN	2,5-STAN
A-45	87.6	24.7	67.7	7.6	21,6	59.3	6.7
A-70	97.6	53.0	39.1	7.9	51.8	38.2	7.7
ADL-H/03	96.1	39.3	53.5	7.2	37.8	51.4	6.9
ADL-i/03	96.9	40.5	52.4	7.2	39.2	50.7	7.0
CT-482	97.0	56.1	36.1	7.8	54.4	35.0	7.6

1.3. HETEROGENEUS CATALYSYS USING ION EXCHANGE RESINS

1.3.1. Fundamentals

The main function of a catalyst is to reduce the activation energy of a chemical process, thus providing an alternative reaction pathway to obtain specific products and resulting in a higher reaction rate at the same temperature, as shown in *Figure 4*. Catalytic reactions are used in many production processes, such as sulphuric acid, fuels, diols, polymers, pharmaceuticals, fragrances, lubricants, etc.

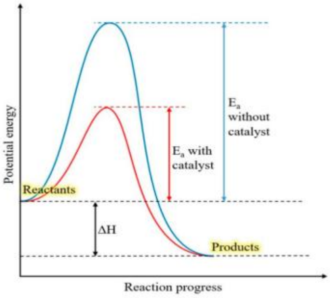

Figure 4. Simplified reaction path diagram without and with the use of a catalyst [18]

However, the importance of catalysis lies in the fact that it is practised in approximately more than 50% of chemical production today. More specifically, heterogeneous catalysis is employed in 80% of these processes at some point.

It should be noted that catalysis with solids prevents several disadvantages mentioned above in relation to homogeneous catalysis, as well as facilitating the recycling of the catalyst, enabling its use in a fixed bed and increasing reaction rates and selectivities. One of the catalytic processes of current interest to improve is the dehydration of sorbitol to different polyols [19] such as propylene glycol, ethylene glycol and isosorbide.

The optimisation of the solid catalyst design is one of the basic objectives when using heterogeneous catalysis in a process. The criteria to be taken into consideration are its chemical, physical, mechanical and catalytic characteristics [20]. The chemical properties correspond to its composition and concentration of active centres. Particle size, particle shape and resistance to attrition are clear examples of physical properties. The activity, selectivity and stability of the solid make up the catalytic properties. Finally, mechanical resistance is an essential quality of an industrially applicable catalyst.

1.3.2. Physicochemical stages of the heterogeneous catalysis

Heterogeneous catalysis involving a solid catalyst in contact with a liquid or gas phase is the most common. Chemical adsorption on the catalyst surface of at least one of the reactants is necessary for this phenomenon to occur, so properties such as the size and volume of the pores, the specific surface area and the specific surface structure become key aspects [21].

However, adsorption is not the only event in the catalytic process, but generally consists of more steps, as described in the following model for porous solid catalysts according to *Figure 5*:

1- External mass transfer (EMT) or diffusion of the reactants from the fluid phase sinus to the external surface of the solid particle.
2- Internal mass transfer (IMT) or diffusion of the reactants through the catalyst pores.
3- Adsorption of the reactants on the active centres.
4- Chemical reaction between adsorbed reactants or between adsorbed species and non-adsorbed molecules located in the fluid phase.
5- Desorption of the products generated in the previous reaction.

6- Internal mass transfer (IMT) or diffusion of the products through the pores to the outer surface of the catalyst.
7- External mass transfer (EMT) or diffusion of the products from the external surface to the surrounding fluid.

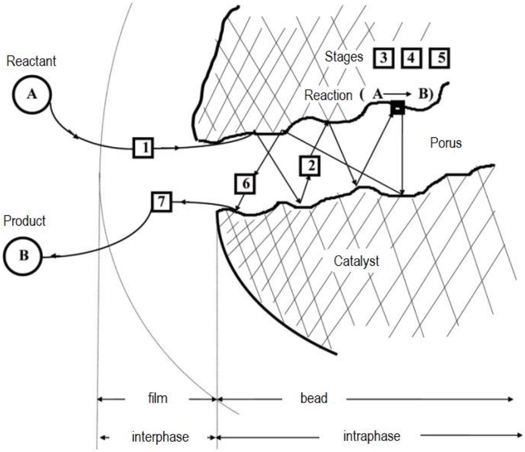

Figure 5. Diagram of the stages of a heterogeneous catalysis process using a porous solid [22]

Stages 3, 4 and 5 are chemical processes that are incorporated in the kinetics of the reaction, although adsorption and desorption at the active centres are usually assumed to be faster stages compared to the chemical reaction. In contrast, the rest correspond to physical diffusion processes in which matter transfer processes take place.

On the one hand, the resistance to external mass transfer will be determined by the film thickness of the solid particles of the resin, which can vary depending on the stirring speed of the reacting system. On the other hand, the internal mass transfer resistance can be studied by varying the particle diameters of the catalyst, taking into account that they share approximately similar geometry.

In order to determine a controlling stage, i.e., one that is much slower than the rest, the study of the velocities of each phase is a common methodology in these mechanisms. In this way, it is possible to consider this controlling step in the kinetic model and neglect the rest. But, in case the internal diffusion velocity is low, the reaction could even occur at the surface of the solid.

Consequently, stages 2 and 6 are considered to occur in series parallel to the rest of the stages, all of them in series [23].

1.3.3. Ion exchange resins as a catalyst

An ion exchange process is a chemical reaction where ions from a solution are removed and replaced with others of a similar electrical charge. Ion Exchange resins (IER) are composed of a matrix of organic polymers forming a three-dimensional network of hydrocarbons chains. Ion exchange sites with the functional groups of cations or anions are ubicated throughout the matrix, attracting ions of opposite charge and acting, consequently, as a physical medium that facilitates ion exchange.

Depending on the type of functional group the resin is equipped with, it can behave in 4 different ways:

- Strong acid cation exchanger (SAC), with a sulphonate as functional group which is usually charged with Na^{2+} ions for softening applications or with H^+ ions for demineralisation processes.
- Weak acid cation exchanger (WAC), including carboxylic acids in the polymer matrix with high affinity towards H^+ ions. They are frequently used for the removal of pH-associated cations.
- Strong base anion exchanger (SBA), with various amine functional group possibilities (e.g. trimethylamine to adsorb chloride ions).
- Weak base anion exchanger (WBA), with the function of acid absorbers removing anions associated with strong mineral acids via ammonium groups.

In addition, these compounds are also widely used in water purification, hydrometallurgy, chromatography, biomolecular separations and acid-base catalysis [24]. As for catalysis, the innovative idea of using such compounds instead of mineral acids and bases was born in 1911 [25]. The adaptability to continuous processes, the easy separation with the solvent and the substitution of corrosive products such as sulphuric acid are some of the advantages mentioned above, as well as the possibility of working in aqueous and non-aqueous media.

Resins in turn can be divided into two main groups according to their structure: gel and macroreticular resins. The gel resin polymer matrix appears homogeneous and without discontinuities on a microscopic scale. In case the resin particles were completely dry, the polystyrene chains are contracted by atomic forces resulting in the collapse of the matrix. Therefore, under these conditions, the bead shows almost no catalytic activity because the active centres inside the particle are not available for the reactants, but only the surface sites are usable [26] . This fact shows the importance in catalysis processes of the reactant's ability to "swell" the matrix of the gel resin. Macroreticular resins, on the other hand, are not affected by this phenomenon due to the macropores that form their structure, through which the reactant circulates without any problem, giving them a wider spectrum of possibilities in the world of catalysis [27].

The two types of structure can be observed in a more visual way in *Figure 6*:

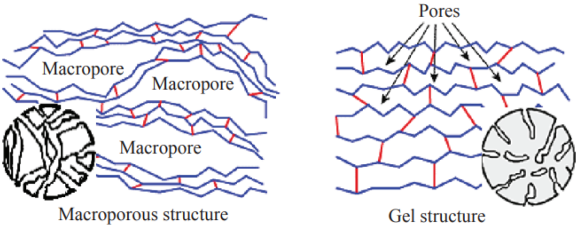

Figure 6. Internal structure of macroporous and gel resins [28]

In summary, the reaction rates provided by a resin vary according to its acidity and the accessibility of the active centres [29].

1.3.4. State of the art

During the last decade, isosorbide has been in the spotlight of the research world thanks to its promising qualities as a substitute for petroleum derivatives. The sulphuric acid in the process is being replaced by another type of solvent, such as water, together with an acid catalyst. As this is a polar aprotic solvent, there is an important tendency in the formation of hydrogen bonds producing a correct solubility of sorbitol, besides being an eco-friendlier compound.

Recently, it has come to light a kinetic investigation of the dehydration of sorbitol to isosorbide using $NbOPO_4$ as a solid catalyst [30], obtaining yields of 65% of the final product at a reaction time of 10 hours and a temperature of 250ºC.

In the present work, CT-482 acid resin is proposed as a catalyst for the process, since in a comparative study of different resins it was possible to obtain yield values similar to those of $NbOPO_4$ but using lower temperatures and reaction times. This fact is due to their characteristics: a small percentage of divinylbenzene (DVB), a wide pore diameter, and a high volume of swelling polymer [17]. In addition, the influence of mass transfer effects that may occur in the experimental set-up during the reaction will be studied.

2. OBJECTIVES

The main aim of this work is to perform a kinetic study on the synthesis of isosorbide via sorbitol dehydration using the resin CT-482. To achieve it, the following subobjectives are established:

- To develop an analytical procedure and to set up the experimental device in which the experimental runs will be carried out.
- To study the effects of the catalyst load, internal and external mass transfers in order to determine the experimental conditions at which the mass transfer resistances can be considered negligible.
- To assess the reactants conversion, selectivity and yield towards the different products at different reaction temperatures and initial concentration of reactant.
- To estimate the experimental reaction rates of formation and consumption of the involved species by derivation of the corresponding mole evolutions, and to infer by comparison of the rate magnitudes, the rate-determining-step (RDS) of the studied system of consecutive reactions.
- To perform an empirical kinetic modelling of the initial formation rates of isosorbide aimed at obtaining a mathematical expression correlating reaction rate with the experimental variables, which enables further interpolation within the range explored.
- Under the premise of the afore mentioned objectives, to elucidate the optimum conditions within the range explored for maximizing the production of isosorbide in terms of catalyst activity and selectivity.

3. EXPERIMENTAL SECTION

3.1. MATERIALS: REACTANTS AND CATALYST

Pure sorbitol (Alfa Aesar, CAS: 50-70-4, 98% purity) was used as starting material and water (Mili-Q, Millipore) was used as solvent. The initial concentration of sorbitol was varied in the range 0,025 – 0,1 g/mL. The amount of solvent was kept constant as 90 mL. It should be noted that a solvent is necessary as the melting temperature of sorbitol is 95ºC, so it would melt in the temperature range worked with.

Nitrogen gas (Abelló Linde, 99.99995 %GC) was used to pressurize the AutoClave reactor to keep the solvent in liquid state at high temperatures, as it evaporates at 100°C.

As for the catalyst, one acidic thermostable cation-exchange resin was used: Purolite CT-482. This resin distinguishes itself by its capacity to operate at high temperatures, up to 190ºC to be precise. *Table 2* shows some of its main properties.

TABLE 2. Characteristics and properties of the ion exchange resin CT-482

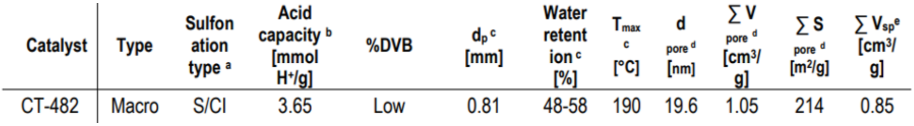

Catalyst	**Type**	**Sulfonation type** [a]	**Acid capacity** [b] **[mmol H^+/g]**	**%DVB**	**d_p** [c] **[mm]**	**Water retention** [c] **[%]**	**T_{max}** [c] **[°C]**	**d_{pore}** [d] **[nm]**	**$\sum V_{pore}$** [d] **[cm^3/g]**	**$\sum S_{pore}$** [d] **[m^2/g]**	**$\sum V_{sp}$** [e] **[cm^3/g]**
CT-482	Macro	S/Cl	3.65	Low	0.81	48-58	190	19.6	1.05	214	0.85

3.2. EXPERIMENTAL SETUP

The dehydration of sorbitol to isosorbide reaction was conducted in a stainless steel (316 SS) stirred batch reactor with 100 mL of capacity (AutoClave Engineers) fitted with a jacket working at 30 bar. The pressure was measured by a manometer incorporated in the system between the relief valve and the reactor with a rupture disc conditioned to release the working pressure in case it exceeded the limits of the device (approx. 50 bar).

A four mixed-up impeller blade in conjunction with a rotor (Magnedrive II Series 0.7501) composed the agitation device. In addition, in order to ensure full homogenisation of the reaction mixture, a baffle was positioned next to the stirrer. A frequency converter model T-VERTER N2 SERIES was responsible for controlling the stirring speed of the system. In purpose to control the temperature inside the vessel, the reactor had a built-in thermocouple which, in turn, was implemented in a PID temperature control system.

The temperature conditioning unit consisted of an electric furnace in the form of a jacket with a temperature reader to measure it. This reading was observable on the temperature control system connected to the system.

Regarding the piping-valves system, the valves numbered 1 to 5 had the function of catalyst injection by means of a pressure difference created by the nitrogen supply. Besides, the V-6 to V-8 valves were used for sampling as explained later in the experimental procedure section. The experimental set-up with all its respective accessories is shown in *Figure* 7.

Finally, for the analysis of the sample, a high-performance liquid chromatography (HPLC) (Infinitty II series, Agilent Technologies Ltd.) with a column (Hi Plex Ca, Agilent Technologies Ltd.) working at a fixed temperature of 80°C and a constant flow rate of 0.3 mL/min of Mili-Q water as a mobile phase was used. It should be noted that the HPLC and the reactor were not connected, so the sample had to be transported.

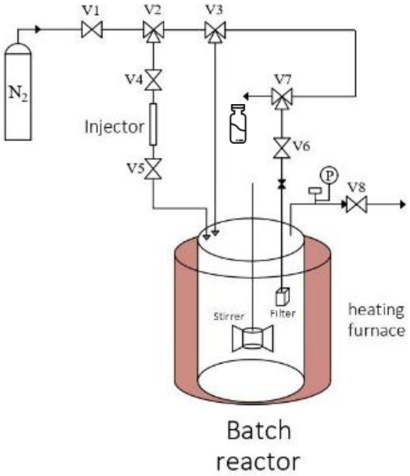

Figure 7. Schematic of the experimental system [17]

3.3. EXPERIMENTAL PROCEDURE

3.3.1. Preparation and execution of the experiments

First of all, the necessary amount of sorbitol (reactant) and water (solvent) were weighted and loaded into the reactor. Then, the reactor was properly closed, the temperature control was set to the desired reaction temperature and the pressure was set 10 bar.

Thereupon, valve V-1 was opened, and valve V-3 was rotated looking up in order to let nitrogen input to the reactor, so it became pressurized. Continuedly, valve V-3 was closed, and the pressure value was around 30 bar due to the regulation valves of the nitrogen system itself. Furthermore, the manometer remained at a constant value indicating good reactor sealing.

In that case, the heating furnace was placed around the reactor and started up together with the agitation system. Once the set point was reached, the catalyst was prepared to be injected. First, the catalyst was removed from the oven after 24 hours at 110°C in order to remove the absorbed moisture. It was then weighed and fed into the injector. During this process, it was required to check that the V-5 valve was kept closed in order to prevent the catalyst from entering the reactant system. Moreover, this step must be carried out quickly due to the high hygroscopic behaviour of the catalyst to prevent it from absorbing humidity and forming a plug in the injector.

The pressure in the reactor should be about 10 bar and the V-8 would have to be opened if it was higher. To ensure a correct introduction of CT-482, a pressure difference of at least 20 bar was required between the nitrogen supply system and the reactor Nevertheless, could not be lower than 10 bar to avoid evaporation of the solvent in the process of opening the valve. With the required pressure in the reactor, the valve V-5 was opened and closed as soon as the reactor reached the pressure of the nitrogen line.

Finally, V-8 was again opened to reach 10 bar and this procedure was repeated at least 5 times. The instant of the first injection was considered to be initial time (t=0) and therefore the start of the reaction time.

3.3.2. Sampling

For sample extraction, V-7 was switched to the left. Then V-6 was slowly opened while the sample was collected in a vial with a hole in it. In this way, the evaporation of part of the sample due to the pressure gap was avoided. It was necessary to extract a little more than 50 microlitres per sample, trying to remove the minimum volume from the device.

Once the sample contained the right amount, V-6 was closed, and V-7 was turned to the right. Then, valve V-8 was opened until the pressure was reduced to about 10 bar. Thereupon, this valve was closed, and v-6 was opened to let nitrogen circulate and recover the solution at the pipe retained by the extraction process. After the reactor pressure equalised with the supply line pressure, the relief valve was closed. This procedure had to be quick to implement in order to avoid considerable variations in temperature that could affect the experimental results.

All these steps were repeated for the extraction of every sample. It is worth noting that the first one was collected just before injecting the catalyst, once the reactor was reached the setpoint temperature to ensure only the presence of the reactant. From the above-named time zero, a sample was extracted every 30 minutes during the first 2.5 hours and every hour until the end of the runs, resulting in a total duration of approximately 6,5 hours.

Then, each sample was subjected to HPLC analysis as described in the previous section injecting it into the device. To avoid saturation of the refractive index detector (RID), every sample was previously diluted 1:2 with water. In some cases, a 1:4 dilution was required.

3.3.3. Clean up

After removing the last sample, the stirring and heating were stopped, the nitrogen feed was stopped by closing V-1 and the reactor was cooled down to room temperature. The pressure was then released from the vessel by opening V-8 and the Autoclave was opened. The remaining reaction volume is subsequently decanted through a pleated filter resulting in the liquid phase in one vial and the resin in another.

To ensure that the catalyst had been fully injected, the nitrogen supply was allowed to pass through and valve 5 was opened and closed rapidly. After an initial rinsing of the stirring accessories and the container with Millipore, the system was filled with this water and properly closed. In order to clean the system internally, the same procedure was followed as for the experimental system. But, of course, no catalyst was injected, and the jacket was set at 50°C.

The extraction of "samples" during the washing allowed a proper cleaning of the filter and the recirculating system consisting of V-6, V-7 and V-8. Finally, after a few hours, the reactor was emptied and dried with pressurised air after a final soaking in Millipore.

A cleaning with water was supposed to be sufficient, in principle, because the species involved in the reaction were very hygroscopic. However, a final pass with acetone was carried out in case there might have been any resin or powder residues left on the device.

3.4. EXPERIMENTAL CONDITIONS

All experiments were carried out at a pressure range between 30 and 40 bar, reaching a reaction time of 6.5 hours with the same resin as catalyst (CT-482).

Different experiments were performed in order to study the effect of the following parameters: particle diameter of the catalyst, agitation, amount of catalyst, temperature and amount of reactant. The study was conducted by altering one of the variables and keeping the other four constant.

Four different particle diameters obtained by sieving with different meshes will be tested: below 0.08 mm, between 0.08 and 0.16 mm; 0.16 and 0.25 mm and, lastly, from 0.25 to 0.4. To study the effect of external mass transfer, 4 experiments were carried out at different stirring speeds: 250, 500, 750 and 1000 rpm.

On the other hand, 3 other experiences were carried out alternating the amount of catalyst to be injected in order to observe its effect on the kinetics. The values were in the range between 0.375 and 1.5 g. In addition, tests were carried out at 5 different temperature values, keeping the temperature constant for each of them from 150 to 190 ºC, for three different initial amounts of sorbitol: 2.25, 4.5 and 9 g. The total number of kinetic runs and the conditions are summarized in *Table 3*. In all these experiences, the amount of catalyst, the stirring speed and the particle diameter were kept constant at values at which the mass transfers were negligible.

TABLE 3. Summary table of design of the experiments free of mass resistances

T [ºC]	m^0_{SOH} [g]
150	2.25
	4.5
	9
160	2.25
	4.5
	9
170	2.25
	4.5
	9
180	2.25
	4.5
	9
190	2.25
	4.5
	9

3.5. CALCULATIONS

As the experimental system is a batch reactor, the conversion is defined by the amount of reactant that has reacted from the beginning of the reaction until a specific time in relation to the initial time, giving rise to the *Equation 1*:

$$X_{SOH}[\%]=\frac{n^0_{SOH}-n_{SOH}(t)}{n^0_{SOH}}\cdot 100 \qquad (1)$$

where n_0^{SOH} are the initial moles of sorbitol and n_{SOH} (t) are the moles of sorbitol at a given time.

The selectivities of the different species involved in the reaction - isosorbide (desired product), 1,4-sorbitan (intermediate product) and 2,5-sorbitan (by-product) - are calculated. The selectivity is defined as the ratio of product mole formed in a certain time to the total mole reacted, as shown in *Equation 2*:

$$S_j[\%] = \frac{n_j(t)}{n_j(t) + n_k(t) + n_l(t)} \cdot 100 \tag{2}$$

where n(t) stands for moles at a particular time and the subscripts j,k and l correspond to the different species formed.

In addition, the products yield was calculated as:

$$Y_j(t)[\%] = S_j(t) \cdot X_{SOH}(t) \tag{3}$$

The contact time has been quantified at each time value in each experiment, defined as described in *Equation 4*, where w_{cat} symbolises the mass on dry basis of the catalyst. In this way, a normalisation of the experimental results of the evolution of the products distribution in the experiments at different conditions is achieved.

$$t_{contact} = \frac{t\ [min] \cdot W_{cat}\ [g]}{n^0_{SOH}} \tag{4}$$

The reaction rate of sorbitol, isosorbide and 2,5-sorbitan is calculated for each time value in each experiment. For this purpose, a regression of the function formed by the mole evolution of each substance with respect to time was performed with the software CurveExpert Professional. The slope of the derivative of the fitted function at each point correspond to the reaction rate.

The sorbitol reaction has been approximated to an exponential and the other two to Exponential Association with two constant parameters.

Finally, with the initial reaction rates of sorbitol and isosorbide, an Arrhenius-like linear regression is performed, *Equation 5*, to estimate the reaction activation energies from the slope.

$$\ln r_j = \frac{-E_{a_j}\ [J/mol]}{R\ [J/(K \cdot mol)]} \cdot \frac{1}{T\ [K]} + \ln A \tag{5}$$

where r is the reaction rate of a species j, indicated as a sub-index, E_a is the corresponding activation energy, R represents the ideal gas constant, T means the temperature and finally, A is the frequency factor.

3.6. MASS BALANCE AND REPRODUCIBILITY CHECK

The fulfilment of the mass balance was computed by a mass balance of carbons at different times with respect to the initial carbon atoms present in the loaded sorbitol as reactant, obtaining a deviation of approximately 11% on average for all the experiments, probably due to errors of experimental origin or possible humins formation.

In order to know the reproducibility of the assays and the experimental error associated with their execution, using the same experimental setup and procedure herein used, a previous work from our research group [17] estimated an experimental error of about 10-15%, and the experiments were considered repeatable.

This experimental uncertainty has been assumed to be identical in the present study and therefore the runs were considered reproducible, as they argued [17] even the error between the replicates was notable, it was similar to that obtained in the carbon balance.

4. RESULTS AND DISCUSSION

4.1. DESCRIPTION OF THE REACTION SYSTEM. MOLE EVOLUTION PROFILES.

The chromatographic areas from the HPLC analysis of the samples taken from every experiment at different instants were translated into mole using the calibration curves of the different compounds in the HPLC carried out in a previous study [17] to the present one, since both use the same instrumentation and conditions for sample analysis (*Appendix 1*).

As mentioned above, the reaction under study is the dehydration of sorbitol to form 1,4-sorbitan (intermediate product) and 2,5-sorbitan, which is a by-product. The reaction culminates in the formation of isosorbide from further dehydration of the intermediate.

Figure 8 clearly illustrates this set of consecutive reactions at two different reaction temperatures representing the lowest (a) and the highest (b) ones within the explored condition. In both cases, a notable decrease of the sorbitol mole is observed with the course of the runs, accompanied by an increase followed by a decrease in the intermediate mole, and finally a steadily increasing mole trend for the target product (isosorbide) and the by-product (2,5-sorbitan). Noteworthy, the decreasing part of the intermediate is not observed at the lowest temperature (a) since the kinetics are much slower at this condition and therefore the mole maximum is not reached during the run.

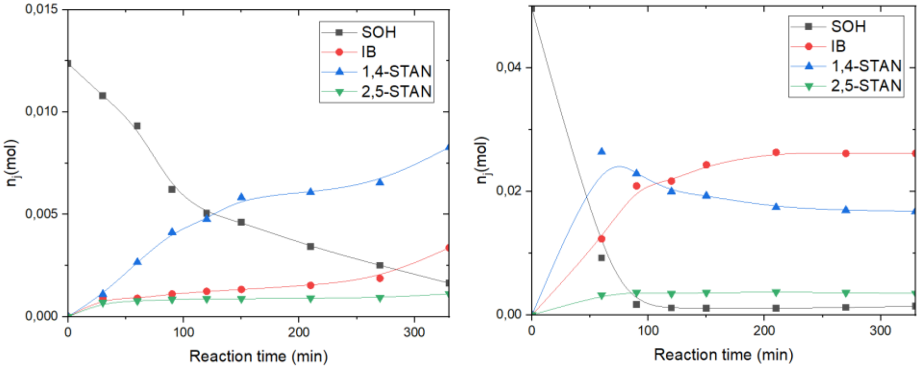

Figure 8. Evolution of the distribution of the number of moles of the species involved in the reaction under the conditions of 750 rpm, dp=0.16 to 0.25 mm, w_{cat}*=0.750 g a) T=150 ºC* m^0_{SOH} *=2,25 g b) T=190 ºC* m^0_{SOH} *=9 g*

4.2. PREMILINARY EXPERIMENTS

In order to determine at which conditions the resistances to mass transfers are negligible in the reaction under study, the effects of catalyst mass loaded to the reactor, and external and internal mass transfers were studied beforehand. All these experiments were carried out at the maximum temperature explored, where the effects are expected to be more noticeable for kinetic reasons.

4.2.1. Effect of catalyst Load

In aim to study the influence of the amount of catalyst on the reaction and to find an optimum measurement in terms of isosorbide formation, experiments were carried out with three different weights: 0.375; 0.750 and 1.5 g. The three experiments were performed at a constant temperature (190°C), initial mass of sorbitol (4.5 g), stirring (750 rpm) and dp (0,16-0.25mm).

The figure below shows the progression of molar concentration of sorbitol and isosorbide versus the contact time. It should be recalled that, following the definition of contact time, it increases with the higher the amount of catalyst.

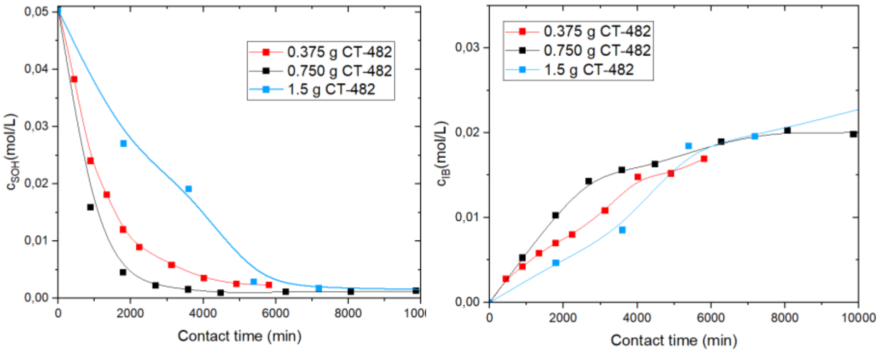

Figure 9. Evolution of the distribution of the molar concentration at different amounts of catalysts of a) sorbitol and b) isosorbide under the conditions of T=190ºC, m^0_{SOH}=4.5g, stirring=750 rpm and dp=0.16-0.25 mm. Lines are guide to the eye.

It is clearly observed that at the intermediate catalyst value there is a higher sorbitol conversion and isosorbide production for the first contact times. Moreover, for this amount of resin the resulting exponential functions are more distinguishable and follow a clearer trend.

In addition, experiments at higher resin amounts show higher values for sorbitol conversion and isosorbide yield at the final reaction time as show in *Table 4*. However, the latter parameter is very low for the smaller amount of catalyst injected. It is evident that the lesser the amount of resin, the lesser the available surface area and, therefore, the active centers catalyzing the reaction are found in a minor abundance.

TABLE 4. Collection of the results of the study of the effect of the amount of catalyst at t=330 min (T=190ºC, m^0_{SOH}=4.5g, stirring=750 rpm and dp=0.16-0.25 mm)

	X [%]	S [%]			Y [%]		
mCT-482(g)	SOH	IB	1,4-STAN	2,5-STAN	IB	1,4-STAN	2,5-STAN
0.375	95.4	35.1	57.3	7.61	33.5	57.3	7.26
0.750	97.7	57.1	34.2	8.73	55.8	34.2	8.53
1.50	97.7	59.9	32.3	7.87	58.5	32.3	7.69

However, for the two highest CT-482 catalyst loads, the difference in terms of final product yield is negligible, so it is assumed that the injected amount of catalyst does not affect the results above a value of 0.750 g.

For all these reasons, this measurement is the one used in the kinetic study of sorbitol dehydration.

4.2.2. Effect of external mass transfer (EMT)

Four tests varying the stirring speed of the system from 250 to 1000 rpm were carried out in order to study the influence of external matter transfer. For all the experiments, the temperature was kept constant at about 190°C, as well as the initial mass of sorbitol and resin (dp=0.16 to 0.25 mm), corresponding to about 4.50 g and 0.750 g respectively.

Figure 10 compiles the evolution of the molar concentration of the reactant (a) and of the desired product (b). It can be seen that the distributions follow a very similar trend with insignificant differences in the experimental set, all the points being close to each value of contact time, some even overlapping.

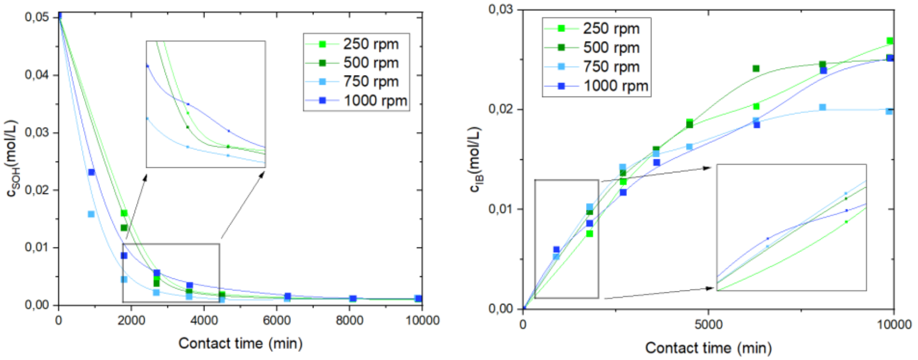

Figure 10. Evolution of the distribution of molar concentration varying the stirring power of a) sorbitol and b) isosorbide. T=190ºC, m^0_{SOH}=4.5g, w_{cat}=0.750 g and dp=0.16-0.25 mm. Lines are guide to the eye

In general, it is known that the higher the stirring speed, the faster the reaction progresses, because the catalyst film becomes thinner and the resistance to external matter transfer is lower. But even if the differences between tests are small, they can be considered non-significant.

At 1000 rpm, higher reactant concentrations and lower product concentrations are observed at initial times than at 750. It is suspected that the discrepancy may be due to the fact that the agitation is so high that a centrifugal force is produced which holds the catalyst on the walls. Thus, the contact area is considerably reduced, and the reaction takes place more slowly.

Therefore, in light of the results obtained, external mass transfer from 750 rpm onwards is assumed negligible. Henceforward, this agitation will be used in the kinetic study of the isosorbide synthesis as it shows higher initial reaction rates.

4.2.3. Effect of internal mass transfer (IMT)

In order to check the influence of internal mass transfer, 4 tests were carried out for different catalyst particle size values, from diameters below 0.08 mm to values between 0.25 and 0.4 mm. As in the case of the EMT control study, the temperature was kept constant at 190°C and the initial mass of sorbitol at 4.5 g for all tests, as well as the agitation, which was maintained at 750 rpm, as the external mass transfer was found to be negligible at this value. In addition, the amount of resin introduced was also the same, 0.750 g.

First of all, the differences in the progression of the evolution of the species concentrations do not appear to be notably significant, except for the smallest resin particle diameter, as illustrated in *Figure 11*:

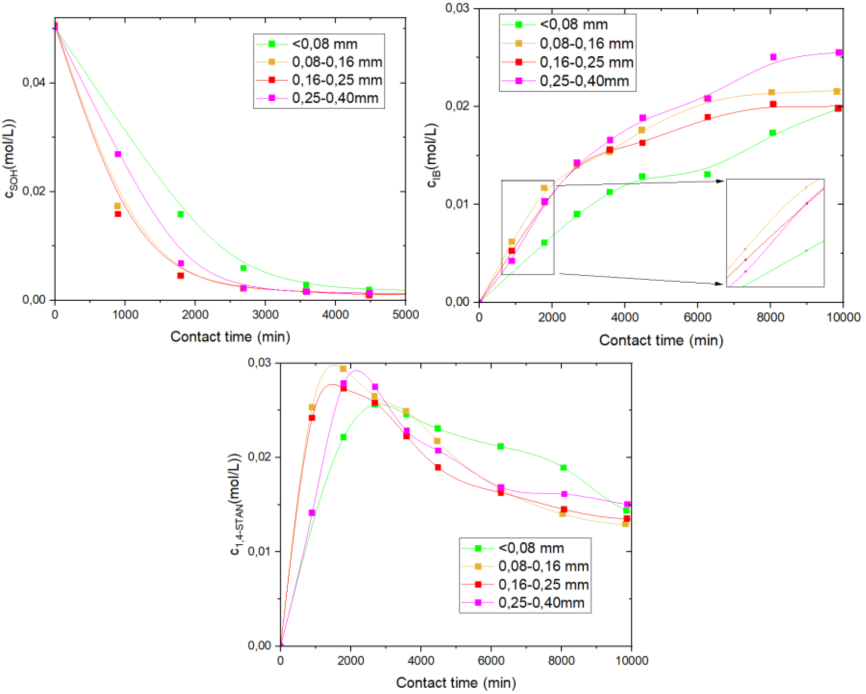

Figure 11. Evolution of the distribution of molar concentration varying the catalyst size of a) sorbitol, b) isosorbide and c) 1,4-sorbitan. T=190ºC, m^0_{SOH}=4.5g, w_{cat}=0.750 g and stirring=750 rpm. Lines are guide to the eye

It stands to reason that the smaller the particle diameter, the faster the diffusion of reactants through the pores, and therefore the internal transfer of mass can be neglected at sufficiently small particle sizes. This phenomenon is clearly observed in the initial contact times.

However, the smallest particle size studied does not follow the expectation and has no physical meaning according to the above explanation. This fact is explained because the fine powder used was more prone to block the injector. Indeed, it was observed during the cleaning that all the catalyst was not injected in this run, which resulted in the lower rates obtained.

At longer contact times, the isosorbide concentration increases, to a small extent, with resin size. The larger the particle size, the more active centres the catalyst molecule contains and therefore, the more species react in the long term.

Ultimately, as the trend shown by the larger particle diameter also separates a little further and the smaller particle diameter cannot be taken into consideration in our experimental set up, it is concluded that at values between 0.08 and 0.25 mm particle diameter, the internal transfer of mass can be considered negligible. In turn, it is decided to use the catalyst with a particle diameter of 0.16 to 0.25 mm for the kinetic study of the reaction.

4.3. KINETIC EXPERIMENTS FREE OF MASS TRANSFER RESISTANCES

4.3.1. Effect of temperature

As mentioned above, experiments have been carried out at 5 different temperature values between 150°C and 190°C for different starting amounts of sorbitol but keeping the values of agitation (750 rpm), catalyst mass (0.750 g) and particle diameter (0.16-0.25 mm) as discussed above.

In order to explain the effect of temperature on the kinetics of the reaction, the results of experiments carried out with an initial amount of 4.50 grams of reactant are discussed and shown in *Table 5:*

TABLE 5. Summary of experimental results of study of temperature effect at t=390 min (m^0_{SOH} = 4.5 g, w_{cat}=0.750 g, stirring=750 rpm and dp=0.16-0.25 mm).

	X [%]	S [%]			Y [%]		
T [ºC]	SOH	IB	1,4-STAN	2,5-STAN	IB	1,4-STAN	2,5-STAN
150	81.7	21.4	71.3	5.93	17.5	58.3	7.26
160	94.9	31.6	61.0	7.00	30.0	57.9	7.00
170	97.4	39.0	50.9	9.91	38.0	49.6	9.91
180	98.3	58.2	32.2	9.42	57.2	31.7	9.59
190	98.6	57.8	33.6	8.48	57.0	33.1	8.48

First of all, a clear increasing trend of sorbitol conversion can be observed with increasing reaction temperature, reaching a value of about 98% for the highest temperatures. By examining *Figure 12*, this tendency can be seen more clearly:

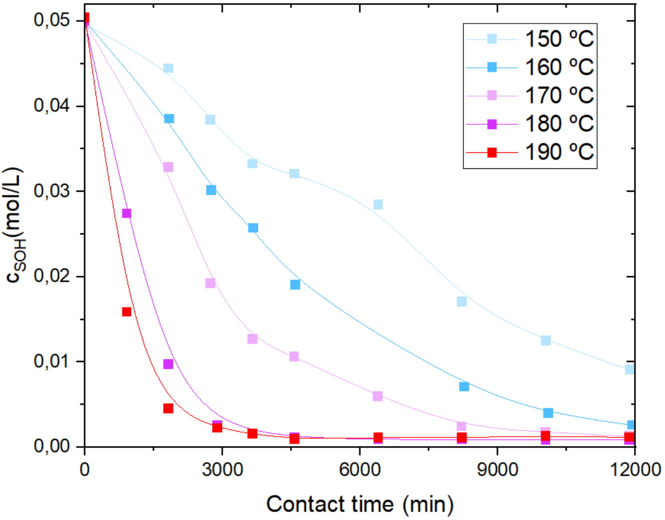

Figure 12. Development of the molar concentration of sorbitol at different temperatures (m^0_{SOH} = 4.5 g, w_{cat}=0.750 g, stirring=750 rpm and dp=0.16-0.25 mm). Lines are guide to the eye

The observed behaviour is as expected, since the higher the temperature, the higher the reaction rate according to the Arrhenius dependence of the kinetic constants. Therefore, increasing temperature produces a greater consumption of reactants, i.e. higher conversion. By analysing the progressions in the figure, it can be deduced that, to obtain the same conversion value, less time is needed at higher temperatures.

In the same way, the performance of 1,4-sorbitan and isosorbide can be explained. By increasing the temperature and reacting more sorbitol, more intermediate product is generated.

But, in addition, the reaction of 1,4-sorbitan consumption to the final product is also favoured by such an increment. The reduced selectivity of sorbitan and the improved selectivity of isosorbide corroborate this fact, reaching values of approximately 58% selectivity and 57% yield of isosorbide. The evolution of the reported behaviour can be noticed in the figure below:

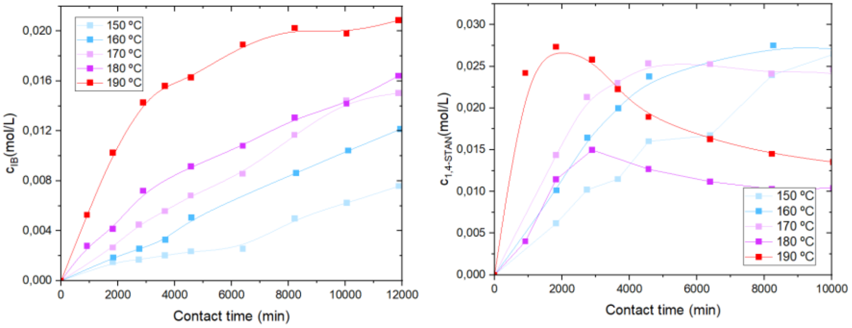

Figure 13. Evolution of the molar concentration at different temperatures of (a) isosorbide and (b) 1,4-sorbitan. (m^0_{SOH} = 4.5 g, w_{cat}=0.750 g, stirring=750 rpm and dp=0.16-0.25 mm). Lines are guide to the eye.

It can also be noted that sorbitol consumption and isosorbide formation at lower temperatures follow an apparently linear behaviour. However, at higher temperatures the trend is more exponential-like. This fact occurs independently of the initial mass of sorbitol, as can be seen in *Appendix* 2. A lower than expected 1,4-sorbitan concentration is also observed in the 180ºC experiment. This phenomenon is due to a somewhat significant deviation in the matter balance.

On the other hand, the formation of 2,5-sorbitan does not seem to follow any trend and varies little compared to the other species.

4.3.2. Effect of initial concentration of sorbitol

As shown in *Table 3*, three different values of initial mass of reactant are used. Experiments at 190°C will be used to account for the effect of the initial amount of sorbitol, although they have been carried out for all the temperature values mentioned in the previous section (*Appendix 1*).

It should be recalled that, in the study of the effect of temperature, the experiments shared approximately the same contact time points. However, the higher the initial amount of sorbitol, the shorter the contact time for the same reaction time.

Figure 14 shows the expected fact that the higher the reactant concentration, the more the reaction is shifted towards the products, so it will go faster. The concentration of sorbitol decreases more drastically the higher the concentration from which it starts. In turn, the formation of isosorbide is also favoured by an increase in the initial mass of reactant. Furthermore, the intermediate product exhibits a progression with a graphically indistinguishable maximum at the smallest concentration of sorbitol, while at the largest concentration this maximum is rapidly exceeded, and its consumption can be mostly observed.

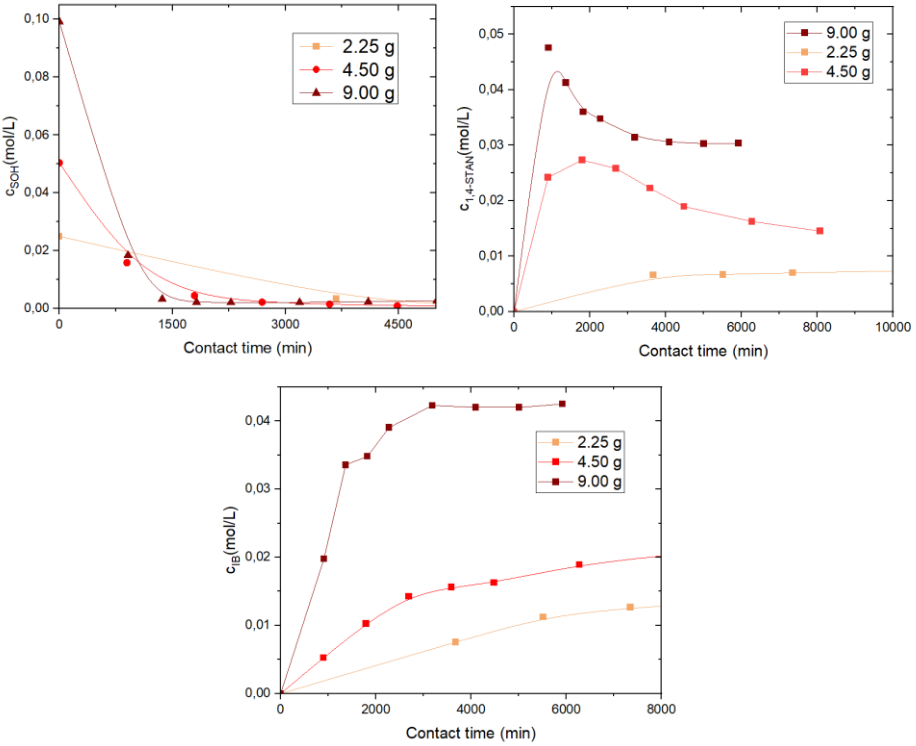

Figure 14. Progression of the molar concentration of (a) sorbitol, b) 1,4-sorbitan and c) isosorbide as a dependence on the initial mass of reactant (T=190ºC, w_{cat}=0.750 g, stirring=750 rpm and dp=0.16-0.25 mm). Lines are guide to the eye

At lower temperatures, the same behaviour as shown in the graph can be observed, but the difference between experiences using the same temperature is not as significant.

It is known that the longer the contact time, the more the reaction moves towards the final product and that this increases as the initial mass of reactant decreases. Therefore, an increment of sorbitol conversion and isosorbide yield are expected at reducing the initial moles of reactant. On the other hand, the same variation will have opposite consequences for the intermediate product, as further progress of the reaction implies more 1,4-sorbitan consumption, so its selectivity and yields will decrease. *Table 6* with the experiments at the most extreme temperatures free of mass transfers demonstrates this result.

TABLE 6. Summary of experimental results of study of mass initial of sorbitol effect at t=390 min. (w_{cat}=0.750 g, stirring=750 rpm and dp=0.16-0.25 mm)

		X [%]	S [%]			Y [%]		
T [ºC]	m^0_{SOH} [g]	SOH	IB	1,4-STAN	2,5-STAN	IB	1,4-STAN	2,5-STAN
150	2.25	86.7	26,4	64.8	8.74	22.9	56.2	7.58
	4.50	81.7	21,4	71.3	7.26	17.5	58.3	5.93
	9.00	76.2	19,1	72.1	8.82	14.5	55.0	6.72
190	2.25	96.1	60.8	28.6	10.56	58.4	27.5	10.1
	4.50	98.6	57.8	33.6	8.48	57.0	33.1	8.48
	9.00	97.0	56.6	36.0	7.46	54.9	34.9	7.23

The behaviour described above is expected for all tests, but this trend is not fully achieved, probably due to errors in the matter balance.

Finally, no clear conclusions can be drawn on the trend of the by-product, although it is also not the subject of study.

4.4. ACTIVATION ENERGY DETERMINATION

A summary of the estimated initial sorbitol consumption and isosorbide formation from derivation of the mole evolution profiles at different experimental conditions is gathered in Table X. As it can be seen, the reaction rate of the second dehydration step is much lower (9 times slower on average depending on the conditions) than that of the first step (including the by-product formation, which must have a small contribution to the total $-r_{SOH}$ estimated given the comparably low 2,5-sorbitan mole detected). Although at first the high initial 2,5-sorbitan rate (*Table 7*) may contradict this fact, at intermediate and final times it undergoes a large drop along with a rapid stabilisation of the number of moles, as illustrated above in *Figure 8*. Therefore, the formation of isosorbide by means of the 1,4-sorbitan dehydration can be considered the rate-determining-step

(RDS). Furthermore, this fact explains why the analyses of matter transfer effects studied above focus mainly on the behaviour of the isosorbide molar concentration distributions.

TABLE 7. Overview of the initial rates of sorbitol consumption and isosorbide formation obtained in the kinetic study (w_{cat}=0.750 g, stirring=750 rpm and dp=0.16-0.25 mm).

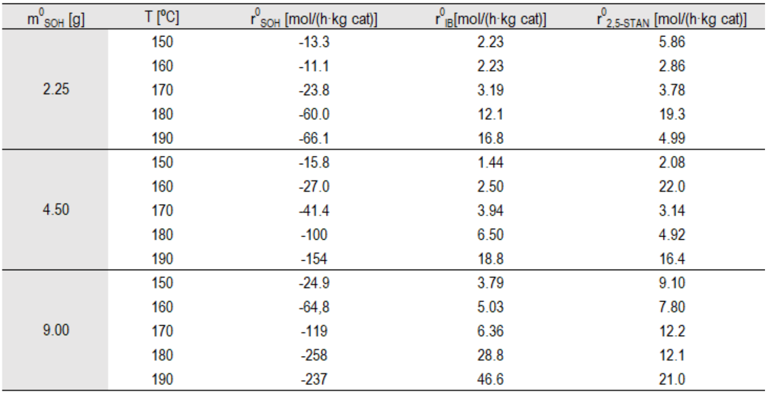

m^0_{SOH} [g]	T [ºC]	r^0_{SOH} [mol/(h·kg cat)]	r^0_{IB}[mol/(h·kg cat)]	$r^0_{2,5\text{-}STAN}$ [mol/(h·kg cat)]
2.25	150	-13.3	2.23	5.86
	160	-11.1	2.23	2.86
	170	-23.8	3.19	3.78
	180	-60.0	12.1	19.3
	190	-66.1	16.8	4.99
4.50	150	-15.8	1.44	2.08
	160	-27.0	2.50	22.0
	170	-41.4	3.94	3.14
	180	-100	6.50	4.92
	190	-154	18.8	16.4
9.00	150	-24.9	3.79	9.10
	160	-64,8	5.03	7.80
	170	-119	6.36	12.2
	180	-258	28.8	12.1
	190	-237	46.6	21.0

Linear regressions for the reactions at different initial masses of initial sorbitol by linearisation of the Arrhenius kinetics (*Equation 5*) are necessary for the estimation of both activation energies, as already mentioned in section 3.5. It should be noted that the activation energy of sorbitol consumption is a combination of the two energies of the reactions in which it participates: formation of 2,5-sorbitan and 1,4-sorbitan, as illustrated in *Figure 8*.

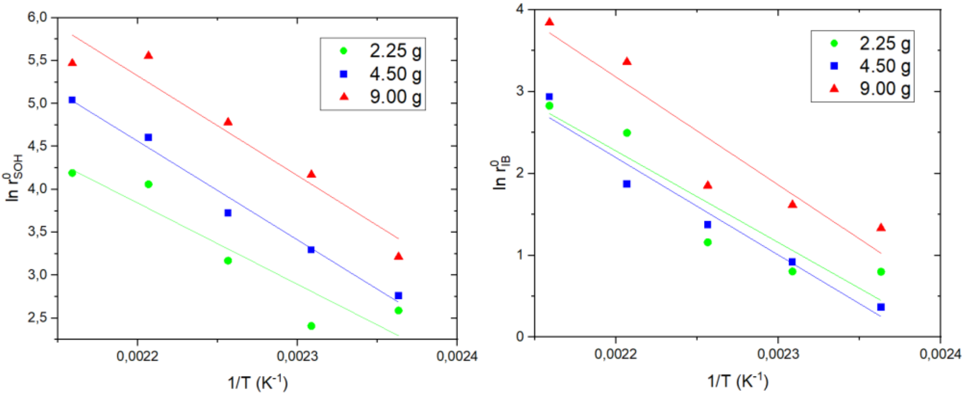

Figure 15. Linear regressions of the Arrhenius equation for the experimental results of the initial reaction velocities for the three amounts of m^0_{SOH} shown in the legend for temperature values from 150 to 190°C (w_{cat}=0.750 g, stirring=750 rpm and dp=0.16-0.25 mm).

As a result, close parallel lines are obtained as a function of the initial amount of sorbitol. The parallelism is logical because the three regressions of each spice should result in the same activation energy value. However, the difference in the independent term is that the pre-exponential Arrhenius factor, also called frequency factor, includes the term for the initial amount of reactant.

Activation energies of 90 ± 10 kJ/mol for sorbitol consumption and 100 ± 18 kJ/mol for isosorbide formation are estimated by averaging the three cases. The values are consistent when comparing the dehydration activation energies of other alcohols as ethanol with an apparent reaction energy between 80 and 105 kJ/mol depending on the sulfonate resin used as catalyst [31].

With comparison purposes, a recent study on the kinetics of the same system using $NbOPO_4$ as catalyst reported an activation energy of 117 kJ/mol for the consumption of sorbitol towards the intermediate, and 138 kJ/mol for the formation of isosorbide by further dehydration [30]. Furthermore, another study that investigated the same process, obtained similar activation energies for isosorbide formation with the SBA-15-Pr-SO3H resin (117 kJ/mol) and larger with H-Beta-19 zeolite (132,8 kJ/mol) used as catalysts [32]. Our values are comparably lower, which along with the lower temperatures used in our study obtaining similar yields to isosorbide, reinforce the potential benefits of using ion-exchange resins, e.g. CT-482, for the present system.

4.5. EMPIRICAL KINETIC MODELLING OF ISOSORBIDE FORMATION RATES

In order to find out to what extent the independent variables, i.e., temperature and initial amount of sorbitol, affect the isosorbide formation, a response surface methodology (RSM) is applied by means of a polynomial multivariable fit. For this purpose, a second-order response surface was used since, for most processes, it provides a sufficiently accurate description of the non-linear relationship between the variables and their corresponding responses [33]. The general equation used also accounting for first order interactions is as follows:

$$y = \beta_0 + \sum_{m=1}^{n} \beta_m z_m + \sum_{m=1}^{n} \beta_{mm} z_m^2 + \sum_{l=1}^{n} \sum_{m=l+1}^{n} \beta_{lm} z_l z_m \qquad (6)$$

where z_1, z_2... z_m are the independent input variables, y is the dependent response variable, and β_0, β_m, β_{mm} and β_{lm} are the regressors.

The software used to carry out this study is DesignExpert13. To assess the statistical significance of the polynomial models obtained by the tool, a confidence level of 95% was adjusted to Fisher's test (F-value). On the other hand, the p-value statistical criterion with a probability level of 95% ($p=0.05$) was used to choose whether including or not the parameters, generating therefore a parsimonious empirical model.

The response variable to be studied was the initial rate of isosorbide formation, obtaining an approximated well-fitted empirical model ($R^2>0.87$), see *Figure 18a*, according to the analysis of variance tool (ANOVA). Given the nature of the residuals a transformation (square root) was used to reduce the heteroscedasticity (increasing magnitude of the residuals with the response) observed [34], which improved the R^2 to 0.93, see *Figure 18b*. The multivariable fitting was performed in terms of coded variables to normalize their different magnitude. The resulting polynomial equation are:

$$r_{IB}^0 = 642.8 - 7.635\,T - 3130\,n_{SOH}^0 + 20.27\,T\,n_{SOH}^0 + 2.257E-2\,T^2 \qquad (7)$$

$$(r_{IB}^0)^{0.5} = 67.26 - 8.034E-1\,T - 360.0\,n_{SOH}^0 + 1.631\,T\,n_{SOH}^0 + 2.492E-3\,T^2 + 1907\,{n_{SOH}^0}^2 \qquad (8)$$

A simpler model only including only the raw variables (T and n^0_{SOH}) was also suggested as feasible. The regressors obtained were both positive, as expected, indicating that reaction rates increase with temperature and initial reactant concentration. However, the capability to predict of such simplified model was notably lower than that herein proposed (*Figure 18b*, *Equation 8*). Even though, some of the regressors in our final model are negative, e.g. T, after a sensitivy analysis considering the interaction between variables included in the model, revealed that increaseing both T and n^0_{SOH}, also resulted in increasing the initial isosorbide formation rates.

Looking at *Figures 16a* and *16b* it can be seen that the points are randomly distributed above and below the value 0. From this fact it can be concluded that both models are well calibrated, i.e. they are neither over- nor under-dimensioned. However, a better repartition of residuals along the x-axis is noticeable in the better model (*Figure 16b*).

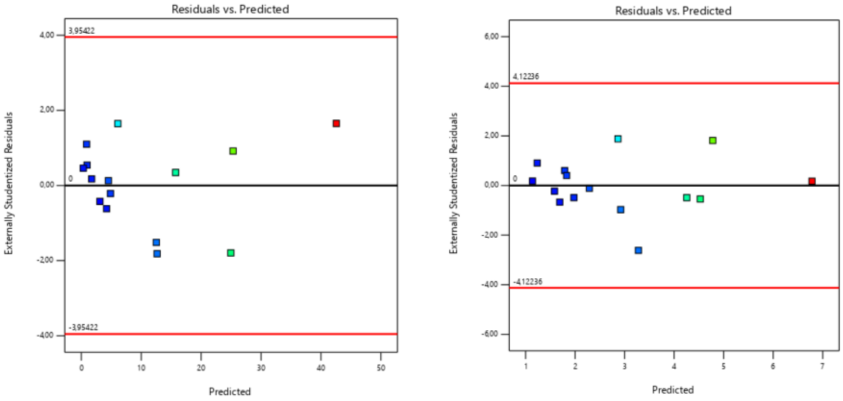

Figure 16. Residual plots of the empirical models corresponding to (a Eq. 8 and (b Eq. 9

A correct distribution of the experimental points with respect to the tabulated ones is observed in the parity plots (*Figures 17a* and *17b*) which confirms a good adequacy of the empirical model.

Although, again, the distribution of the points is cleaner in the modelage with higher R^2 (*Equation 8*, *Figure 18b*).

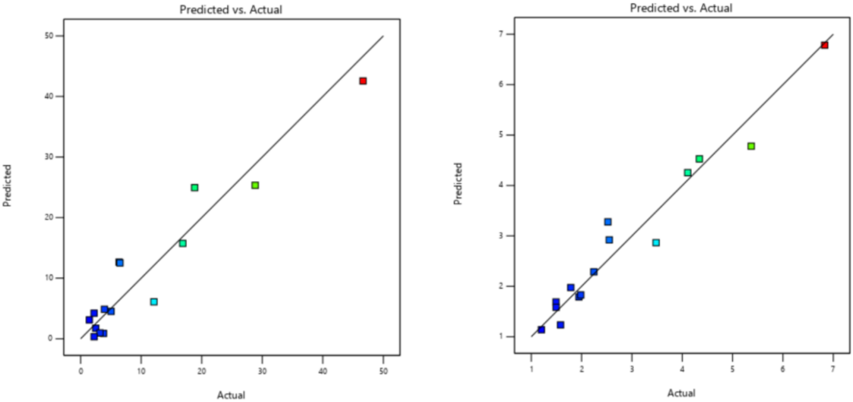

Figure 17. Parity plots of the empirical models corresponding to (a Eq. 8 and (b Eq. 9

As mentioned above and according to the Arrhenius model, the higher the temperature, the higher the reaction rate. In addition, information on the contribution of the initial amount of sorbitol to the model as a function of the reaction temperature can be extracted from *Figure 18b*. The influence of the amount of starting reactant on the rate of formation of the final product at low temperatures is hardly discernible but, as the temperature increases, it becomes more relevant giving rise to much higher rates. The maximum value of the initial rate of isosorbide formation is clearly distinguishable at higher values of the both input variables.

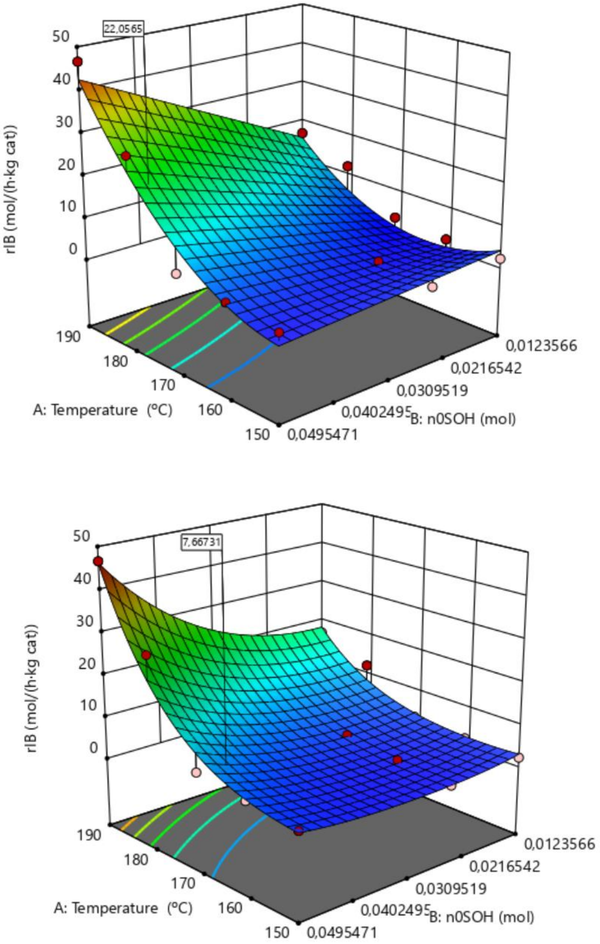

Figure 18: Result of the empirical model expressed by (a) equation 7 and by (b) equation 8 in the range of input variables studied

Finally, it is to be noted that the proposed empirical model is useful for predicting (interpolating) initial isosorbide formation rates free of mass transfers avoiding the need for conducting additional experiments as long as the experimental variables are within the range explored.

5. CONCLUSIONS

It can be concluded that all the sub-objectives described above have been met. The experiments have been successful, confirming that it has been possible to establish a correct experimental methodology and a correct set-up of the instrumentation.

It has been evaluated the influence of mass transfers as well as that of catalyst loading, obtaining a range of values for which these effects could be considered practically negligible. Thus, the kinetic study of the double dehydration of sorbitol as a function of temperature and initial reactant concentration free of mass transfer effects was feasible, obtaining a maximum isosorbide selectivity value of 60% at the highest temperature used (190ºC) and at the lowest amount of sorbitol initial mass (2.25 g).

In addition, activation energies of 90 ± 10 kJ/mol for sorbitol consumption and 100 ± 18 kJ/mol for isosorbide formation were obtained from the initial formation rates estimated from the derivation of the evolution of the moles of these species. These energies are smaller than those found in the most recent literature, so it is concluded that CT-482 resin is a good catalyst. Furthermore, observing that the initial isosorbide formation is significantly slower than the consumption of sorbitol, considering that the contribution of 2,5-sorbitan formation is of little relevance in view of its low concentration values, it is determined that the rate-determining step (RDS) is the second dehydration, i.e., isosorbide formation from the intermediate product.

It is also concluded that the empirical modelling of the initial isosorbide formation rate as a function of temperature and initial moles of reactant is adequate for the process carried out in our experimental setup, allowing an interpolation within the range of experimental values used in this work. This model clearly shows the initial maximum rate of isosorbide formation at the highest temperature (190°C) and the highest number of initial moles (9.00 g), as expected from Arrhenius kinetics.

A search for the highest isosorbide yield based on initial reaction rate and selectivity as a function of initial reactant mass is suggested for future study objects.

REFERENCES AND NOTES

[1] C.B. Field, J.E. Campbell, D.B. Lobell, Biomass energy: the scale of the potential resource, Trends in Ecology and Evolution. 23 (2008) 65–72. https://doi.org/10.1016/J.TREE.2007.12.001.

[2] P. McKendry, Energy production from biomass (part 1): Overview of biomass, Bioresource Technology. 83 (2002) 37–46. https://doi.org/10.1016/S0960-8524(01)00118-3.

[3] J. Müller, U. Hoffmann, Verfahren zur Darstellung von hochwertigen Alkoholen durch katalytische Reduktion von Zuckerarten mit Wasserstof., DE Patent 544 666, 1925.

[4] H. Li, W. Li, Z. Guo, D. Gu, S. Cai, A. Fujishima, The Paired Electrochemical Synthesis of Gluconic Acid and Sorbitol, Collection of Czechoslovak Chemical Communications. 60 (1995) 928–934. https://doi.org/10.1135/CCCC19950928.

[5] K.D. Barrow, J.G. Collins, D.A. Leight, P.L. Rogers, R.G. Warr, Sorbitol production by Zymomonas mobilis, Applied Microbiology and Biotechnology. 20 (1984) 225–232. https://doi.org/10.1007/BF00250630.

[6] J.R. Ochoa-Gómez, T. Roncal, Production of Sorbitol from Biomass, (2017) 265–309. https://doi.org/10.1007/978-981-10-4172-3_9.

[7] T. Werpy, G. Petersen, Top Value Added Chemicals from Biomass, U.S. Department of Energy. 1 (2004) 76. https://doi.org/10.2172/926125.

[8] J.J. Bozell, G.R. Petersen, Technology development for the production of biobased products from biorefinery carbohydrates—the US Department of Energy's "top 10" revisited, Green Chemistry. 12 (2010) 539–55. https://doi.org/10.1039/B922014C.

[9] F. Fenouillot, A. Rousseau, G. Colomines, R. Saint-Loup, J.P. Pascault, Polymers from renewable 1,4:3,6-dianhydrohexitols (isosorbide, isomannide and isoidide): A review, Progress in Polymer Science (Oxford). 35 (2010) 578–622. https://doi.org/10.1016/J.PROGPOLYMSCI.2009.10.001.

[10] Global Isosorbide Market Size | Industry Report, 2019-2025, (n.d.). https://www.grandviewresearch.com/industry-analysis/isosorbide-industry (accessed June 7, 2022).

[11] C. Dussenne, T. Delaunay, V. Wiatz, H. Wyart, I. Suisse, M. Sauthier, Synthesis of isosorbide: An overview of challenging reactions, Green Chemistry. 19 (2017) 5332–5344. https://doi.org/10.1039/C7GC01912B.

[12] M. Yabushita, H. Kobayashi, A. Shrotri, K. Hara, S. Ito, A. Fukuoka, Sulfuric acid-catalyzed dehydration of sorbitol: Mechanistic study on preferential formation of 1,4-sorbitan, Bull Chem Soc Jpn. 88 (2015) 996–1002. https://doi.org/10.1246/BCSJ.20150080.

[13] US6689892B2 - Process for the manufacture of anhydro sugar alcohols with the assistance of a gas purge - Google Patents, (n.d.). https://patents.google.com/patent/US6689892B2/en (accessed May 30, 2022).

[14] J. Xia, D. Yu, Y. Hu, B. Zou, P. Sun, H. Li, H. Huang, Sulfated copper oxide: An efficient catalyst for dehydration of sorbitol to isosorbide, Catalysis Communications. 12 (2011) 544–547. https://doi.org/10.1016/J.CATCOM.2010.12.002.

[15] H. Kobayashi, H. Yokoyama, B. Feng, A. Fukuoka, Dehydration of sorbitol to isosorbide over H-beta zeolites with high Si/Al ratios, Green Chemistry. 17 (2015) 2732–2735. https://doi.org/10.1039/C5GC00319A.

[16] M.J. Ginés-Molina, R. Moreno-Tost, J. Santamaría-González, P. Maireles-Torres, Dehydration of sorbitol to isosorbide over sulfonic acid resins under solvent-free conditions, Applied Catalysis A: General. 537 (2017) 66–73. https://doi.org/10.1016/J.APCATA.2017.03.006.

[17] L. Castro, M. Iborra, J. Tejero, A contribution to the study of the fructose to isosorbide conversion reaction, 2022.

[18] S.I.S. Mashuri, M.L. Ibrahim, M.F. Kasim, M.S. Mastuli, U. Rashid, A.H. Abdullah, A. Islam, N. Asikin-Mijan, Y.H. Tan, N. Mansir, N.H.M. Kaus, T.Y.Y. Hin, Photocatalysis for organic wastewater treatment: From the basis to current challenges for society, Catalysts. 10 (2020) 1–29. https://doi.org/10.3390/CATAL10111260.

[19] B. Blanc, A. Bourrel, P. Gallezot, T. Haas, P. Taylor, Starch-derived polyols for polymer technologies: Preparation by hydrogenolysis on metal catalysts, Green Chemistry. 2 (2000) 89–91. https://doi.org/10.1039/A909131I.

[20] O. Levenspiel, J. Wiley, Chemical Reaction Engineering Third Edition, (1999).

[21] H. Yokoyama, H. Kobayashi, J.Y. Hasegawa, A. Fukuoka, Selective Dehydration of Mannitol to Isomannide over Hβ Zeolite, ACS Catalysis. 7 (2017) 4828–4834. https://doi.org/10.1021/ACSCATAL.7B01295.

[22] E.E. Gonzo, BASIC CONCEPTS ON TRANSPORT AND TRANSFORMATION PHENOMENA IN HETEROGENEOUS CATALYSIS, (2011).

[23] A. Chakrabarti, M.M. Sharma, Cationic ion exchange resins as catalyst, Reactive Polymers. 20 (1993) 1–45. https://doi.org/10.1016/0923-1137(93)90064-M.

[24] S.D. Alexandratos, Ion-Exchange resins: A retrospective from industrial and engineering chemistry research, Industrial and Engineering Chemistry Research. 48 (2009) 388–398. https://doi.org/10.1021/IE801242V.

[25] W. Neier, Ion exchangers as catalysts, Ion Exchangers. (2011) 981–1028. https://doi.org/10.1515/9783110862430.981.

[26] A.R. Pitochelli, Ion Exchange Catalysis and Matrix Effects, (1980).

[27] US3037052A - Catalyzing reactions with cation exchange resin - Google Patents, (n.d.). https://patents.google.com/patent/US3037052A/en (accessed June 3, 2022).

[28] M.B. Fathi, B. Rezai, E.K. Alamdari, R.D. Alorro, Mechanism and equilibrium modeling of Re and Mo adsorption on a gel type strong base anion resin, Russian Journal of Applied Chemistry. 90 (2017) 1504–1513. https://doi.org/10.1134/S1070427217080208.

[29] D.C. Sherrington, P. (Philip) Hodge, Syntheses and separations using functional polymers, (1988) 454.

[30] L. Wang, X. Liu, Y. Wang, W. Sun, L. Zhao, Thermodynamics and Reaction Kinetics of the Sorbitol Dehydration to Isosorbide Using NbOPO4 as the Catalyst, (2022).

[31] B.C. Gates, L.N. Johanson, The dehydration of methanol and ethanol catalyzed by polystyrene sulfonate resins, Journal of Catalysis. 14 (1969) 69–76. https://doi.org/10.1016/0021-9517(69)90357-1.

[32] G. Morales, J. Iglesias, J.A. Melero, J. Moreno, R. Sánchez-Vázquez, Á. Peral, A. Cubo, Isosorbide Production from Sorbitol over Heterogeneous Acid Catalysts: Screening and Kinetic Study, Topics in Catalysis. 60 (2017) 1027–1039. https://doi.org/10.1007/S11244-017-0794-0.

[33] R.H. Myers, D.C. Montgomery, C.M. Anderson-Cook, Response surface methodology, New Jersey, 2009.

[34] G.E.P. Box, ; D R Cox, An Analysis of Transformations, Journal of the Royal Statistical Society. Series B (Methodological). 26 (1964) 211–252.

ACRONYMS

SOH	Sorbitol
IB	Isosorbide
1,4-STAN	1,4-sorbitan
2,5-STAN	2,5-sorbitan
n_j	Moles of compound j
c_j	Molar concentration of compound j
X_{SOH}	Conversion
S_j	Selectivity of product j
Y_j	Yield of product j
t	Time
THF	Tetrahidrofuran
EMT	External mass transfer
IMT	Internal mass transfer
IER	Ion exchange resins
SAC	Strong acid cation
WAC	Weak acid cation
SBA	Strong base anion
WBA	Weak base anion
RDS	Rate-determining step
HPLC	High-performance liquid chromatography
RID	Refractive index detector
w_{cat}	Mass of catalyst

r_j	Reaction rate of species j
E_{aj}	Activation energy of the reaction of compound j
RSM	Response surface methodology
DVB	Divinylbenzene

APPENDICES

APPENDIX 1: CALIBRATION OF HPLC

CALIBRATION HPLC EQUATIONS [17]

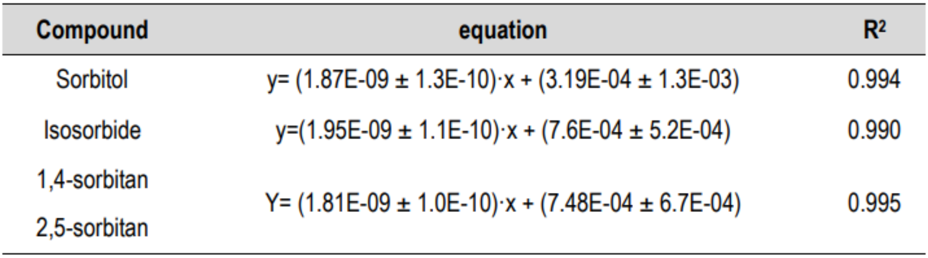

Compound	**equation**	**R^2**
Sorbitol	$y= (1.87E-09 \pm 1.3E-10)\cdot x + (3.19E-04 \pm 1.3E-03)$	0.994
Isosorbide	$y=(1.95E-09 \pm 1.1E-10)\cdot x + (7.6E-04 \pm 5.2E-04)$	0.990
1,4-sorbitan	$Y= (1.81E-09 \pm 1.0E-10)\cdot x + (7.48E-04 \pm 6.7E-04)$	0.995
2,5-sorbitan		

APPENDIX 2: PRELIMINARY STUDY

EXP 24: IMT EFFECT

$m_{CT\text{-}482}$ [g]	0,748	Temperature [ºC]	190
m_{SOH} [g]	4,578	Stirring [rpm]	750
m_{H2O} [g]	90,28	dp [mm]	0,08-0,16

t [min]	n_j [mol]			
	SOH	IB	1,4-STAN	2,5-STAN
0	0,0251	0	0	0
30	0,0086	0,0038	0,0139	0,0018
60	0,0022	0,0072	0,0162	0,0020
90	0,0010	0,0086	0,0146	0,0020
120	0,0008	0,0095	0,0137	0,0021
150	0,0005	0,0109	0,0120	0,0021
210	0,0005	0,0129	0,0092	0,0020
270	0,0005	0,0133	0,0077	0,0020
330	0,0004	0,0133	0,0071	0,0019
390	0,0006	0,0138	0,0073	0,0020

EXP 25: IMT EFFECT

$m_{CT\text{-}482}$ [g]	0,751	Temperature [ºC]	190
m_{SOH} [g]	4,577	Stirring [rpm]	750
m_{H2O} [g]	90,77	dp [mm]	0,16-0,25

t [min]	n_j [mol]			
	SOH	IB	1,4-STAN	2,5-STAN
30	0,0251	0	0	0
60	0,0079	0,0033	0,0134	0,0016
90	0,0022	0,0064	0,0151	0,0019
120	0,0011	0,0089	0,0143	0,0020
150	0,0008	0,0097	0,0123	0,0020
210	0,0005	0,0101	0,0105	0,0019
270	0,0006	0,0118	0,0090	0,0020
330	0,0006	0,0126	0,0080	0,0019
390	0,0006	0,0123	0,0075	0,0019
450	0,0006	0,0130	0,0078	0,0020

EXP 26: IMT EFFECT

$m_{CT\text{-}482}$ [g]	0,751	Temperature [ºC]	190
m_{SOH} [g]	4,57	Stirring [rpm]	750
m_{H2O} [g]	91,02	dp [mm]	0,25-0,4

t [min]	n_j [mol]			
	SOH	IB	1,4-STAN	2,5-STAN
0	0,0251	0	0	0
30	0,0134	0,0026	0,0078	0,0012
60	0,0034	0,0064	0,0154	0,0019
90	0,0011	0,0089	0,0152	0,0022
120	0,0008	0,0103	0,0127	0,0021
150	0,0007	0,0117	0,0115	0,0021
210	0,0006	0,0130	0,0093	0,0021
270	0,0004	0,0156	0,0089	0,0023
330	0,0004	0,0159	0,0083	0,0022
390	0,0004	0,0162	0,0081	0,0022

EXP 27: IMT EFFECT

m_{CT-482} [g]	0,75	Temperature [ºC]	190
m_{SOH} [g]	4,576	Stirring [rpm]	750
m_{H2O} [g]	91,14	dp [mm]	<0,08

t [min]	n_j [mol]			
	SOH	IB	1,4-STAN	2,5-STAN
0	0,0251	0	0	0
60	0,0079	0,0038	0,0123	0,0016
90	0,0030	0,0056	0,0142	0,0018
120	0,0014	0,0070	0,0137	0,0019
150	0,0009	0,0080	0,0128	0,0020
210	0,0008	0,0082	0,0118	0,0019
270	0,0007	0,0108	0,0105	0,0020
330	0,0005	0,0123	0,0080	0,0020
390	0,0005	0,0138	0,0078	0,0016

EXP 29: EMT EFFECT

m_{CT-482} [g]	0,752	Temperature [ºC]	190
m_{SOH} [g]	4,573	Stirring [rpm]	250
m_{H2O} [g]	90,45	dp [mm]	0,16-0,25

t [min]	n_j [mol]			
	SOH	IB	1,4-STAN	2,5-STAN
0	0,0251	0	0	0
60	0,0067	0,0061	0,0148	0,0019
90	0,0019	0,0085	0,0167	0,0022
120	0,0011	0,0100	0,0147	0,0022
150	0,0008	0,0115	0,0129	0,0022
210	0,0006	0,0150	0,0106	0,0023
270	0,0006	0,0153	0,0101	0,0023
330	0,0006	0,0157	0,0099	0,0023
390	0,0005	0,0153	0,0094	0,0022

EXP 30: EMT EFFECT

$m_{CT\text{-}482}$ [g]	0,751	Temperature [ºC]	190
m_{SOH} [g]	4,573	Stirring [rpm]	500
m_{H2O} [g]	90,9	dp [mm]	0,16-0,25

t [min]	n_j [mol]			
	SOH	IB	1,4-STAN	2,5-STAN
0	0,0251	0	0	0
60	0,0080	0,0047	0,0128	0,0017
90	0,0025	0,0079	0,0173	0,0022
120	0,0011	0,0099	0,0160	0,0023
150	0,0009	0,0116	0,0157	0,0024
210	0,0007	0,0126	0,0120	0,0022
270	0,0005	0,0148	0,0108	0,0021
330	0,0005	0,0167	0,0098	0,0021
390	0,0005	0,0171	0,0093	0,0024

EXP 35: EMT EFFECT

$m_{CT\text{-}482}$ [g]	0,754	Temperature [ºC]	190
m_{SOH} [g]	4,575	Stirring [rpm]	1000
m_{H2O} [g]	90,41	dp [mm]	0,16-0,25

t [min]	n_j [mol]			
	SOH	IB	1,4-STAN	2,5-STAN
0	0,0251	0	0	0
30	0,0115	0,0037	0,0153	0,0017
60	0,0043	0,0053	0,0156	0,0019
90	0,0028	0,0072	0,0164	0,0021
120	0,0017	0,0091	0,0160	0,0022
210	0,0008	0,0114	0,0124	0,0021
270	0,0006	0,0148	0,0107	0,0023
330	0,0006	0,0156	0,0096	0,0023
390	0,0006	0,0163	0,0090	0,0023

EXP 32: CATALYST LOAD EFFECT

$m_{CT\text{-}482}$ [g]	0,374	Temperature [ºC]	190
m_{SOH} [g]	4,573	Stirring [rpm]	750
m_{H2O} [g]	90,23	dp [mm]	0,16-0,25

t [min]	n_j [mol]			
	SOH	IB	1,4-STAN	2,5-STAN
0	0,0251	0	0	0
30	0,0190	0,0017	0,0099	0,0013
60	0,0119	0,0026	0,0110	0,0014
90	0,0090	0,0036	0,0142	0,0017
120	0,0059	0,0043	0,0148	0,0018
150	0,0044	0,0049	0,0150	0,0018
210	0,0029	0,0067	0,0166	0,0020
270	0,0017	0,0091	0,0181	0,0023
330	0,0012	0,0094	0,0162	0,0021
390	0,0012	0,0105	0,0171	0,0023

EXP 33: CATALYST LOAD EFFECT

$m_{CT\text{-}482}$ [g]	1,504	Temperature [ºC]	190
m_{SOH} [g]	4,572	Stirring [rpm]	750
m_{H2O} [g]	90,9	dp [mm]	0,16-0,25

t [min]	n_j [mol]			
	SOH	IB	1,4-STAN	2,5-STAN
0	0,0251	0	0	0
30	0,0135	0,0029	0,0094	0,0013
60	0,0095	0,0053	0,0133	0,0017
90	0,0014	0,0115	0,0164	0,0023
120	0,0009	0,0122	0,0141	0,0022
210	0,0007	0,0159	0,0103	0,0023
270	0,0006	0,0194	0,0105	0,0025
330	0,0007	0,0196	0,0106	0,0026
390	0,0006	0,0192	0,0103	0,0025

APPENDIX 3: KINETIC STUDY DATA

EXP 37: 150°C, 4,5GSOH

$m_{CT\text{-}482}$ [g]	0,754	Temperature [ºC]	150
m_{SOH} [g]	4,508	Stirring [rpm]	750
m_{H2O} [g]	90,91	dp [mm]	0,16-0,25

t [min]	n_j [mol]			
	SOH	IB	1,4-STAN	2,5-STAN
0	0,0247	0	0	0
60	0,0222	0,0009	0,0034	0,0008
90	0,0192	0,0011	0,0057	0,0009
120	0,0166	0,0013	0,0064	0,0010
150	0,0160	0,0015	0,0089	0,0011
210	0,0142	0,0016	0,0093	0,0011
270	0,0085	0,0031	0,0133	0,0014
330	0,0062	0,0039	0,0146	0,0015
390	0,0045	0,0047	0,0157	0,0016

EXP 38: 150°C, 9GSOH

$m_{CT\text{-}482}$ [g]	0,755	Temperature [ºC]	150
m_{SOH} [g]	9,012	Stirring [rpm]	750
m_{H2O} [g]	90,07	dp [mm]	0,16-0,25

	n_j [mol]			
	SOH	IB	1,4-STAN	2,5-STAN
0	0,0495	0	0	0
30	0,0437	0,0018	0,0038	0,0016
60	0,0391	0,0021	0,0059	0,0017
90	0,0354	0,0020	0,0087	0,0017
210	0,0251	0,0028	0,0143	0,0020
290	0,0213	0,0040	0,0210	0,0024
330	0,0174	0,0050	0,0215	0,0025
390	0,0118	0,0050	0,0189	0,0023

EXP 39: 160°C, 2,25 GSOH

$m_{CT\text{-}482}$ [g]	0,754	Temperature [ºC]	160
m_{SOH} [g]	2,253	Stirring [rpm]	750
m_{H2O} [g]	90,75	dp [mm]	0,16-0,25

t [min]	n_j [mol]			
	SOH	IB	1,4-STAN	2,5-STAN
0	0,0124	0	0	0
60	0,0099	0,0011	0,0031	0,0008
90	0,0070	0,0012	0,0042	0,0009
120	0,0068	0,0015	0,0057	0,0010
150	0,0057	0,0018	0,0065	0,0010
210	0,0039	0,0023	0,0076	0,0011
270	0,0027	0,0029	0,0083	0,0012
330	0,0020	0,0029	0,0076	0,0011
390	0,0013	0,0030	0,0070	0,0011

EXP 40: 160ºC, 4,5 G_{SOH}

$m_{CT\text{-}482}$ [g]	0,753	Temperature [ºC]	170
m_{SOH} [g]	2,254	Stirring [rpm]	750
m_{H2O} [g]	90,77	dp [mm]	0,16-0,25

t [min]	n_j [mol]			
	SOH	IB	1,4-STAN	2,5-STAN
0	0,0247	0	0	0
60	0,0190	0,0011	0,0056	0,0010
90	0,0149	0,0016	0,0090	0,0012
120	0,0127	0,0020	0,0110	0,0013
150	0,0094	0,0031	0,0130	0,0014
270	0,0035	0,0053	0,0151	0,0017
330	0,0020	0,0064	0,0149	0,0017
390	0,0013	0,0075	0,0144	0,0017

EXP 41: 160ºC, 9 G_{SOH}

$m_{CT\text{-}482}$ [g]	0,751	Temperature [ºC]	160
m_{SOH} [g]	9,013	Stirring [rpm]	750
m_{H2O} [g]	90,56	dp [mm]	0,16-0,25

t [min]	n_j [mol]			
	SOH	IB	1,4-STAN	2,5-STAN
0	0,0495	0	0	0
30	0,0407	0,0019	0,0081	0,0017
60	0,0313	0,0027	0,0149	0,0022
90	0,0251	0,0036	0,0195	0,0024
120	0,0188	0,0051	0,0221	0,0026
150	0,0145	0,0056	0,0221	0,0027
210	0,0090	0,0070	0,0231	0,0028
270	0,0056	0,0109	0,0292	0,0033
330	0,0037	0,0125	0,0285	0,0034
390	0,0025	0,0154	0,0287	0,0036

EXP 42: 170ºC, 2,25 GSOH

$m_{CT\text{-}482}$ [g]	0,753	Temperature [ºC]	170
m_{SOH} [g]	2,254	Stirring [rpm]	750
m_{H2O} [g]	90,77	dp [mm]	0,16-0,25

t [min]	n_j [mol]			
	SOH	IB	1,4-STAN	2,5-STAN
0	0,0124	0	0	0
60	0,0067	0,0014	0,0048	0,0009
90	0,0043	0,0023	0,0072	0,0011
120	0,0026	0,0025	0,0077	0,0012
150	0,0017	0,0030	0,0079	0,0012
210	0,0010	0,0039	0,0076	0,0012
270	0,0006	0,0051	0,0073	0,0013
330	0,0005	0,0058	0,0067	0,0013
390	0,0004	0,0063	0,0062	0,0013

EXP 43: 170ºC, 4,5 GSOH

$m_{CT\text{-}482}$ [g]	0,753	Temperature [ºC]	170
m_{SOH} [g]	4,508	Stirring [rpm]	750
m_{H2O} [g]	90,56	dp [mm]	0,16-0,25

t [min]	n_j [mol]			
	SOH	IB	1,4-STAN	2,5-STAN
0	0,0247	0	0	0
60	0,0163	0,0016	0,0079	0,0011
90	0,0095	0,0028	0,0118	0,0014
120	0,0063	0,0034	0,0127	0,0015
150	0,0053	0,0042	0,0140	0,0016
210	0,0030	0,0053	0,0139	0,0016
270	0,0012	0,0072	0,0133	0,0017
330	0,0009	0,0089	0,0136	0,0019
390	0,0006	0,0093	0,0122	0,0024

EXP 44: 170ºC, 9 GSOH

$m_{CT\text{-}482}$ [g]	0,7570	Temperature [ºC]	170
m_{SOH} [g]	9,0020	Stirring [rpm]	750
m_{H2O} [g]	90,26	dp [mm]	0,16-0,25

t [min]	n_j [mol]			
	SOH	IB	1,4-STAN	2,5-STAN
0	0,0494	0	0	0
30	0,0261	0,0021	0,0079	0,0020
60	0,0171	0,0034	0,0155	0,0022
90	0,0135	0,0050	0,0212	0,0026
120	0,0081	0,0057	0,0202	0,0027
150	0,0057	0,0065	0,0188	0,0025
210	0,0040	0,0083	0,0205	0,0028
270	0,0016	0,0128	0,0198	0,0030
330	0,0014	0,0147	0,0182	0,0031
390	0,0011	0,0164	0,0154	0,0031

EXP 46: 180°C, 4,5 g_{SOH}

m_{CT-482} [g]	0,7540	Temperature [ºC]	180
m_{SOH} [g]	4,5100	Stirring [rpm]	750
m_{H2O} [g]	90,21	dp [mm]	0,16-0,25

t [min]	n_j [mol]			
	SOH	IB	1,4-STAN	2,5-STAN
0	0,0248	0	0	0
30	0,0136	0,0017	0,0022	0,0014
60	0,0048	0,0026	0,0063	0,0011
95	0,0013	0,0044	0,0082	0,0014
150	0,0005	0,0056	0,0070	0,0014
210	0,0005	0,0067	0,0061	0,0014
270	0,0004	0,0081	0,0057	0,0015
330	0,0004	0,0088	0,0057	0,0016
390	0,0004	0,0101	0,0056	0,0017

EXP 47: 180°C, 9 g_{SOH}

m_{CT-482} [g]	0,7590	Temperature [ºC]	180
m_{SOH} [g]	9,0120	Stirring [rpm]	750
m_{H2O} [g]	90,04	dp [mm]	0,16-0,25

t [min]	n_j [mol]			
	SOH	IB	1,4-STAN	2,5-STAN
0	0,0495	0	0	0
30	0,0330	0,0046	0,0214	0,0022
60	0,0074	0,0077	0,0229	0,0026
90	0,0018	0,0146	0,0247	0,0032
120	0,0010	0,0158	0,0192	0,0031
150	0,0009	0,0212	0,0187	0,0036
210	0,0007	0,0217	0,0163	0,0036
270	0,0007	0,0226	0,0166	0,0038
330	0,0007	0,0224	0,0158	0,0037
390	0,0007	0,0232	0,0164	0,0039

EXP 48: 190°C, 2,25 G_{SOH}

m_{CT-482} [g]	0,7570	Temperature [ºC]	190
m_{SOH} [g]	2,2510	Stirring [rpm]	750
m_{H2O} [g]	90,09	dp [mm]	0,16-0,25

t [min]	n_j [mol]			
	SOH	IB	1,4-STAN	2,5-STAN
0	0,0124	0	0	0
60	0,0017	0,0047	0,0036	0,0011
90	0,0004	0,0069	0,0037	0,0013
120	0,0004	0,0078	0,0039	0,0014
210	0,0004	0,0092	0,0042	0,0016
270	0,0004	0,0091	0,0042	0,0015
330	0,0004	0,0091	0,0041	0,0015
390	0,0005	0,0087	0,0041	0,0015

EXP 49: 190°C, 9 G_{SOH}

m_{CT-482} [g]	0,7520	Temperature [ºC]	190
m_{SOH} [g]	9,0260	Stirring [rpm]	750
m_{H2O} [g]	90,97	dp [mm]	0,16-0,25

t [min]	n_j [mol]			
	SOH	IB	1,4-STAN	2,5-STAN
0	0,0495	0	0	0
60	0,0092	0,0123	0,0264	0,0032
90	0,0017	0,0209	0,0229	0,0036
120	0,0011	0,0217	0,0200	0,0034
150	0,0010	0,0243	0,0193	0,0036
210	0,0011	0,0263	0,0174	0,0037
270	0,0012	0,0262	0,0169	0,0036
330	0,0014	0,0261	0,0168	0,0035
390	0,0015	0,0265	0,0168	0,0035

EXP 52: 150ºC, 2,25 G_{SOH}

m_{CT-482} [g]	0,7500	Temperature [ºC]	150
m_{SOH} [g]	2,2540	Stirring [rpm]	750
m_{H2O} [g]	90,94	dp [mm]	0,16-0,25

t [min]	n_j [mol]			
	SOH	IB	1,4-STAN	2,5-STAN
0	0,0124	0	0	0
30	0,0108	0,0009	0,0011	0,0007
60	0,0093	0,0009	0,0027	0,0008
90	0,0062	0,0011	0,0041	0,0008
120	0,0051	0,0012	0,0048	0,0009
150	0,0046	0,0013	0,0058	0,0009
210	0,0034	0,0015	0,0061	0,0009
270	0,0025	0,0019	0,0065	0,0009
330	0,0016	0,0034	0,0083	0,0011

EXP 53: 180ºC, 2,25G_{SOH}

m_{CT-482} [g]	0,7510	Temperature [ºC]	180
m_{SOH} [g]	2,2510	Stirring [rpm]	750
m_{H2O} [g]	90,43	dp [mm]	0,16-0,25

t [min]	n_j [mol]			
	SOH	IB	1,4-STAN	2,5-STAN
0	0,0124	0	0	0
30	0,0048	0,0024	0,0043	0,0018
60	0,0018	0,0032	0,0054	0,0021
90	0,0013	0,0049	0,0055	0,0022
120	0,0009	0,0058	0,0047	0,0022
155	0,0007	0,0060	0,0039	0,0021
210	0,0007	0,0061	0,0035	0,0021
270	0,0007	0,0070	0,0035	0,0022
330	0,0006	0,0064	0,0032	0,0022
390	0,0006	0,0064	0,0030	0,0021